AD NUMBER
AD011680
CLASSIFICATION CHANGES
TO: unclassified
FROM: restricted
LIMITATION CHANGES
TO: Approved for public release, distribution unlimited
FROM: Distribution authorized to U.S. Gov't. agencies and their contractors; Foreign Government Information; 23 MAR 1950. Other requests shall be referred to British Embassy, 3100 Massachusetts Avenue, NW, Washington, DC 20008.
AUTHORITY
DSTL, DSIR 23/18876, 18 Nov 2008; DSTL, DSIR 23/18876, 18 Nov 2008

AD-

111680

RESTRICTED

AERONAUTICAL RESEARCH COUNCIL

Two-dimensional Control Characteristics.

- by -

L. W. Bryant, B.Sc., A.R.C.S., A. S. Halliday, B.Sc., Ph.D.,
and A. S. Batson, B.Sc.,
of the Aerodynamics Division, N.P.L.

23rd March, 1950.

Summary.

The design of lifting surfaces for aeroplanes depends fundamentally on two-dimensional data for the aerofoil sections, with flaps where necessary for control. Data of this kind are required for the use of designers, and for the development of methods of calculating control characteristics and stability derivatives for finite wings. Researches on the lift, pitching-moments, and hinge-moments of aerofoils with plain flaps have been carried out at the National Physical Laboratory at a Reynolds number of about 10^6. The results of the experiments have been presented in a generalised form, which shows promise of being applicable over a wide field. The generalised curves have been tested as far as possible from other sources, including some tests made on one of the N.P.L. sections in a R.A.E. Tunnel at Reynolds numbers up to nearly 10^7. It appears that a suggestion due to Preston that the ratio of experimental lift slope ($dC_l/d\alpha = a_1$) to the theoretical value $(a_1)_T$, corresponding to the Joukowsky condition of flow past the trailing-edge, provides a criterion giving the combined effects of Reynolds number, transition points, and aerofoil shape on $dC_l/d\alpha$, and is a very useful starting-point for the estimation of control characteristics. The generalised charts in this report are intended for the estimation of hinge-moment and pitching moment derivatives from the flap-chord ratio, Z, after $a_1/(a_1)_T$ has been determined from a special figure. The latter figure (Fig.12) is a key to the whole process, and it would appear to be very desirable to improve its accuracy and usefulness by further experiments on two-dimensional lift-slopes of thin wings at high Reynolds numbers.

Part I.- The Variation of Lift Coefficient with Incidence.

1. Introduction.

1.1. In a series of papers [1,2,3], (1946-3) Preston originated a method of co-ordinating experimental results relating to plain hinged flaps which showed promise of considerable usefulness. The experimental values of a_1, a_2, b_1, b_2 are expressed as ratios of the corresponding theoretical values for potential flow, $(a_1)_T$, $(a_2)_T$, $(b_1)_T$, $(b_2)_T$, the circulation in the potential flow being that for which the Joukowsky condition at the trailing edge is fulfilled. It is argued that these

theoretical/

2. Theoretical Slope of the Lift-Incidence Curve $(a_1)_T$

The thickness-chord ratio is the principal parameter which determines $(a_1)_T$, whilst there are small variations depending upon the curvature of the leading edge and upon the trailing edge angle or trailing edge curvature. An approximate formula due to H. C. Garner has been found accurate enough for use in control estimations, viz:

$$\frac{(a_1)_T}{2\pi} = c_0$$

where $C_0 = \dfrac{8\,(y_{0.25} + y_{0.75}) + \sqrt{6\rho_L} + \sqrt{6\rho_T}}{6\sqrt{3}}$

or alternatively

$$C_0 = \frac{8\,(y_{0.25} + y_{0.75}) + \sqrt{6\rho_L} + 0.1540 \tan \tau/2}{10.392} \qquad (1)$$

Here $y_{0.25}$ is the half ordinate of the profile at the quarter-chord point.

$y_{0.75}$ is the half ordinate of the profile at the three-quarter-chord point

ρ_L is the radius of curvature at the leading edge

ρ_T is the radius of curvature at the trailing edge

τ is the trailing edge angle.

In Fig.1 are plotted values of $\dfrac{(a_1)_\infty}{2\pi}$ as a function of t/c the thickness-chord ratio, for two families of related aerofoil sections. This may provide sufficient information for an estimate of $(a_1)_T$ in many cases.

3 Experiments on "two-dimensional" models at the N.P.L.

3.1. A series of tests have been made at the N.P.L. (7 ft. No.2 tunnel) in which the lift, among other quantities, has been measured on a 15% thick wing with its maximum ordinate at 41% from the leading edge. The rear portion of the wing has been systematically modified so as to give a range of trailing edge angles from 0° to 28°. Reynolds number is of the order 10^6. The transition point has been varied in position from 0.1 to 0.65 of the chord from the leading edge by means of wires. In addition the transition was allowed to occur, without wires, between 0.65 and 0.7 chord. The gap at the hinge was either extremely small or sealed with grease in all the experiments.

The/

The sections are drawn in Figs.2, 3. They will be referred to as the 154.1 series. The trailing edge angles (τ) were approximately:

Section	154.1 a	154.1 basic	154.1 b	154.1 c	154.1 d
τ	19.2°	15°	9.4°	4.5°	Cusp.

The cusp was designed so that the derivatives up to d^3y/dx^3 were all zero, and in the manufacture a very thin boxwood trailing edge was fitted.

The method of test is described in Part III.

3.2. The experimental results from the 7 ft. tunnel are plotted as ratios $a_1/(a_1)_\tau$ in Fig.12 for two positions of the transition (0.1 and 0.5) as fixed by suitable wires. The errors in the measured slopes appear to be of the order $\pm 1\frac{1}{2}\%$. Included in the same figure are curves from data given in reports from the N.A.C.A. and from tests in the Compressed Air Tunnel at the N.P.L. These additional curves are commented on in Section 4.

3.3. Section 154.1a, trailing-edge angle 19.2°. Fig.2.

All the measurements of a_1 are collected in Fig.4 and plotted against position of transition. There appear to be two groups of results, and the upper, represented by the full line, are believed to correspond to the condition of unbroken surface and no trace of boundary layer separation, either laminar or turbulent. Accordingly values from this curve are plotted on the curves of Fig.7 which gives what are believed to be the best estimates of a_1 in terms of transition for Reynolds number 10^6. When the flap is 40% chord (set at 0° and gap sealed) the values of a_1 corresponding to the dotted curve of Fig.4 were almost invariably measured, and the reason for this had not been found when the investigation had to be discontinued. All later work with smooth surface up to at least 75% of the chord from the leading edge confirmed the higher values which have been accepted.

3.4. Section 154.1, trailing-edge angle 15°. Fig.2.

The results for this section (see Fig.5) are similar to those for 154.1a with lower values when the surface was broken at the hinge of the 40% flap, and the full line values for smaller flaps. The latter are used for plotting on Fig.7.

3.5. Sections with small trailing-edge angles, 154.1b,c,d. Fig.3.

The results for these sections are plotted in Fig.6 the full lines of Figs.4 and 5 being reproduced as well in this figure. In the case of 154.1b there is still the same tendency to low values with the 40% flap, as indicated in Fig.7 where the size of flap is given with most of the observation points plotted. In section 154.1c the difference between 20% and 40% flap models is negligible, and apparently non-existent with the cusped aerofoil.

3.6./

3.6. The curve A of Fig.7 represents the value of the lift curve slope as a function of trailing edge angle when transition occurs at 0.1c on both surfaces, the surfaces are smooth up to well behind 60% chord, and there is no separation of the boundary layer. Similarly curve B represents the lift curve slope for transition at half-chord or beyond. Curve C gives the curve for a_1 taken from Reference 4, which is said to be based mainly on tests at Reynolds numbers between 3 and 4 x 10^6. The slopes were taken over much larger angle ranges than those determined for this report and they probably represent conditions of fair forward transition on the upper surface, and considerably back on the lower. The accuracy claimed being only ±5% curve C may be considered roughly to agree with the results of curves A and B even after making allowance for Reynolds number and for variations of aerofoil thickness.

4. The Effect of Reynolds Number on the Slope of the Lift-Incidence Curve.

4.1. One of the 1541 aerofoils, (1541a), has been tested in the R.A.E. No.2 11½ by 8 ft. Tunnel over a range of Reynolds numbers, 2.5 to nearly 10 x 10^6. The values of $a_1/(a_1)_T$ derived from these tests for transition positions of 0.1 and 0.5c are plotted against Reynolds number in Fig.11. On the same figure are plotted the values of $a_1/(a_1)_T$ deduced from a number of N.A.C.A. tests of two-dimensional models, Ref.5, which had trailing-edge angles of approximately 20 deg. In some cases it was stated in Ref.5 that the tests were made with "leading-edge of standard roughness"; otherwise the position of the transition point was presumably some distance back from the leading-edge. On Fig.11 are plotted also a few points derived from tests of rectangular wings of aspect-ratio 5 in the Compressed Air Tunnel at the National Physical Laboratory over a range of Reynolds numbers; these experimental results were corrected for aspect-ratio by using the empirical formula due to H. C. Garner:

$$a/(a_1)_{eff.} = \text{[illegible]} + \text{[illegible]}\,(a_1/6) \qquad (2)$$

where $(a_1)_{eff.}$ is the measured lift slope. Each plotted point is labelled with a number specifying 100 times the thickness-chord ratio of the section, and those points for which transition is likely to be well forward are distinguished from the remainder for which transition is unknown.

4.2. Similar plottings of $a_1/(a_1)_T$ against Reynolds number are given in Figs. 8, 9 and 10 for aerofoils with trailing-edge angles in the neighbourhood of 5, 10 and 15 degrees respectively. The data are taken from N.A.C.A. sources (Refs. 5, 6 and other reports), from Compressed Air Tunnel tests, as well as from the 1541 series tests in the N.P.L. 7 ft. Tunnel. On each of the figures 8, 9, 10 and 11, full line curves are drawn enclosing between them the majority of the plotted points. These curves were drawn so that cross plotting against trailing-edge angle yielded smooth curves as in Fig.12. In this figure the cross plottings from the data of Figs. 8 to 11 are shown for the upper and lower limiting curves, for the lowest and highest Reynolds numbers of test, viz: 10^6 and 10^7.

4.3/

4.3. After Figs. 8 to 12 were drawn, further data from Ref.6 were examined, and the upper and lower limiting curves for Reynolds number 6×10^6 plotted in Fig.12. The agreement with the limiting curves of Figs. 8 to 11 is excellent.

4.4. The results for the 1941 series (Reynolds number 10^6) are included in Fig.12 and are distinguished by the two dotted curves for the two transition positions 0.1c and 0.5c. It will be noted that, when the trailing-edge angle τ is 20 deg., there is agreement between the upper limiting curve (Reynolds number = 10^6) and the 1941 tests with backward transition. When τ is small there is good agreement between the lower limiting curve and the 1941 data with forward transition. It is concluded that the lower limiting curves of Figs. 8 to 12 would correspond to far forward positions of the transition point, whilst the upper limiting curves apply to transitions well back. Where τ is small the upper limit applies to thinner sections; it is probable that this limit should be lower for thick sections. Where transition is fairly definitely known it seems likely that $a_1/(a_1)_T$ can be estimated within ±2% but where transition is unknown the estimate may be in error by ±5%.

A further interesting feature of the 1941a tests in the R.A.E. Tunnel (see Figs.11 and 12) is the evidence that at the highest Reynolds number, about 10^7, the lift slope, corrected for compressibility effects, agrees with the lower limiting curve from the general data. The value from the R.A.E. Tunnel definitely corresponds to a transition well forward on the upper surface in the neighbourhood of 0.08c.

4.5. Table 1 has been compiled with a view to suggesting a procedure for using Fig.12 for determining $a_1/(a_1)_T$ in a given case, thickness chord ratio, trailing-edge angle and Reynolds number being known. The Table suggests likely values for Reynolds numbers 10^6, 6×10^6, and 10^7, trailing-edge angles 5, 10, 15 and 20 deg., and thickness-chord ratios 0.09 and 0.15, values being estimated for two extreme positions of the transition point. It is thought that Table 1 represents the available data sufficiently well for general use, although greater precision is highly desirable if the subsequent control calculations are to be as reliable as possible.

4.6. Further model experiments needed.

In view of the basic importance of the quantity $a_1/(a_1)_T$, it is a matter of some urgency that further tests should be carried out with the specific purpose of determining lift slopes related to well-defined conditions, so that the chart Fig.12 may be better established. A range of Reynolds numbers should be covered, transition should be observed and controlled where necessary to give sufficient variation, and the sections chosen for test should be such as will supply the required number of key points on the chart. The main weakness lies in the region of small values of τ, and more data on thin sections in general is needed. In order that the conditions determining lift slope should be better understood, some attempt to measure displacement thicknesses of the boundary-layers in the region of the trailing-edge with greater accuracy than has hitherto been achieved is very much to be recommended. Accuracy is required in these measurements because it is a differential effect between the upper and lower boundary-layers which is important in relation to the measured lift in any given case.

Table 1/

TABLE 1.

Values of $a_1/(a_1)_T$

Trailing-edge Angle (degrees)	Transition forward						Transition back					
	t/c ≈ 0.09			t/c ≈ 0.15			t/c ≈ 0.09			t/c ≈ 0.15		
	R = 10^6	6×10^6	10^7	R = 10^6	6×10^6	10^7	R = 10^6	6×10^6	10^7	R = 10^6	6×10^6	10^7
0	0.825	0.90	0.92	[illegible]	[illegible]	[illegible]	0.92			0.86	[illegible]	[illegible]
5	0.80	0.865	0.885	[illegible]	[illegible]	[illegible]	0.835	0.97	0.99	0.84	[illegible]	[illegible]
10	0.78	0.83	0.85	0.76	0.815	0.835	0.85	0.925	0.95	0.82	0.90	0.92
15	0.76	0.80	0.82	0.75	0.79	0.815	0.82	0.89	0.915	0.805	0.875	0.90
20	0.74	0.77	0.79	0.70	0.765	0.79	0.79	0.86	0.89	0.79	0.85	0.88

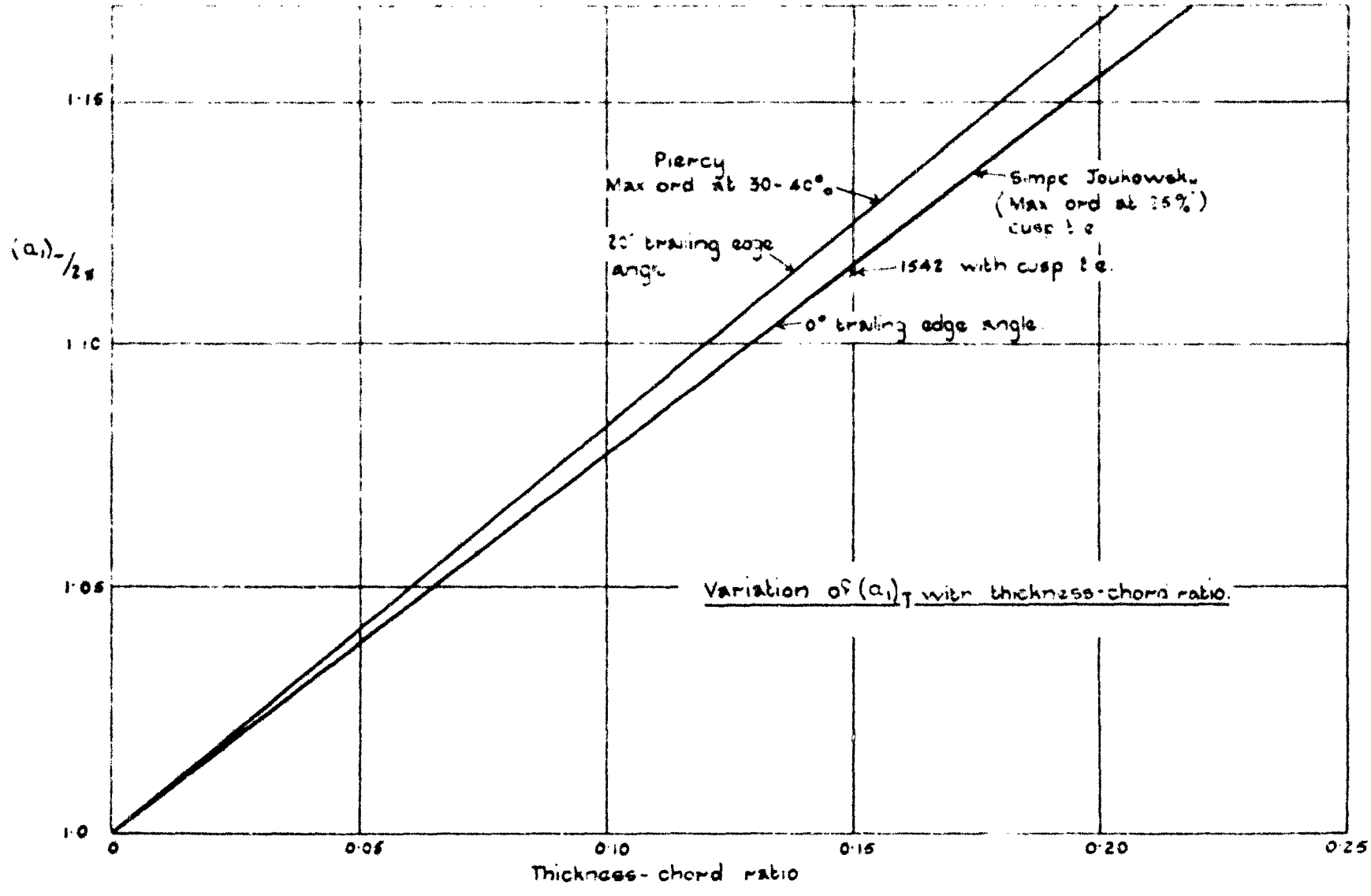
1·15
1·1
1·05
1·0
$(a_1)_T/_{2\pi}$
Piercy
Max ord at 30-40%
20° trailing edge angle
Simpe Joukowski
(Max ord at 25%)
cusp t.e
1542 with cusp t.e.
0° trailing edge angle
Variation of $(a_1)_T$ with thickness-chord ratio.
0
0·05
0·10
0·15
0·20
0·25
Thickness-chord ratio

15 039
FIG 1

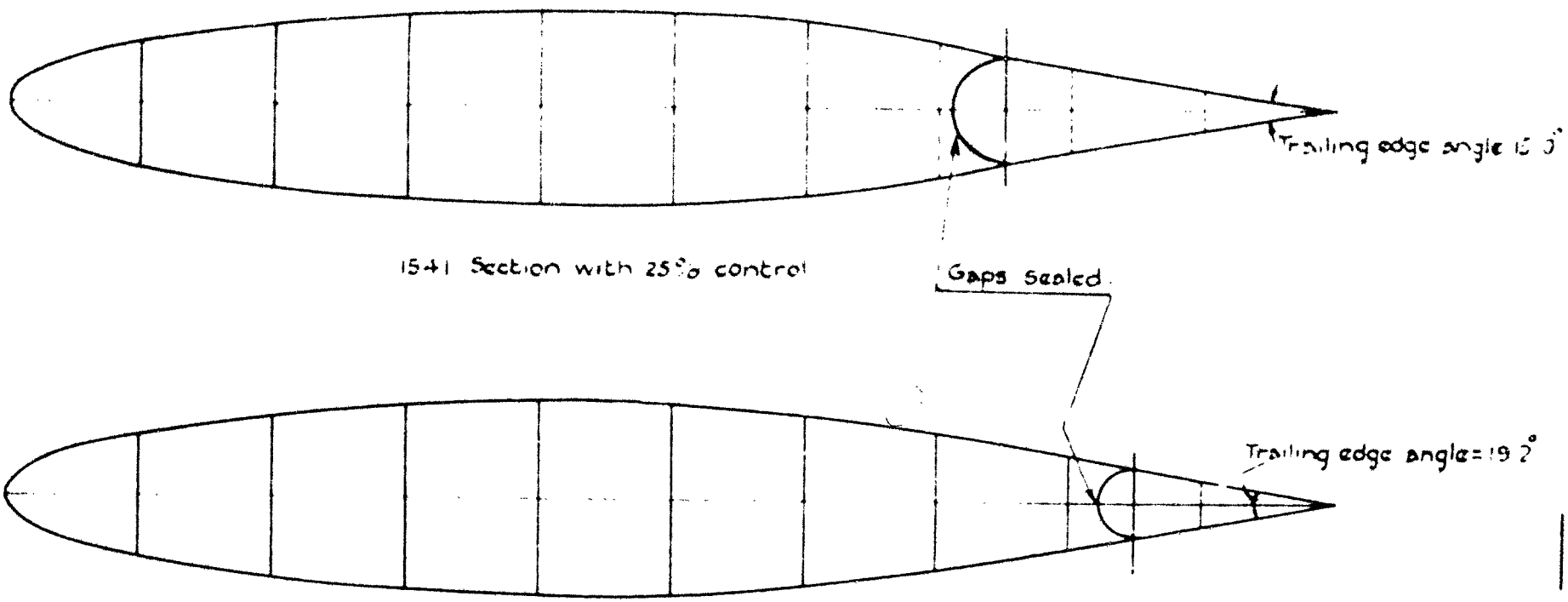

1541 Section with 25% control

1541a Section with 15% flat control.

13,039
Fig. 2

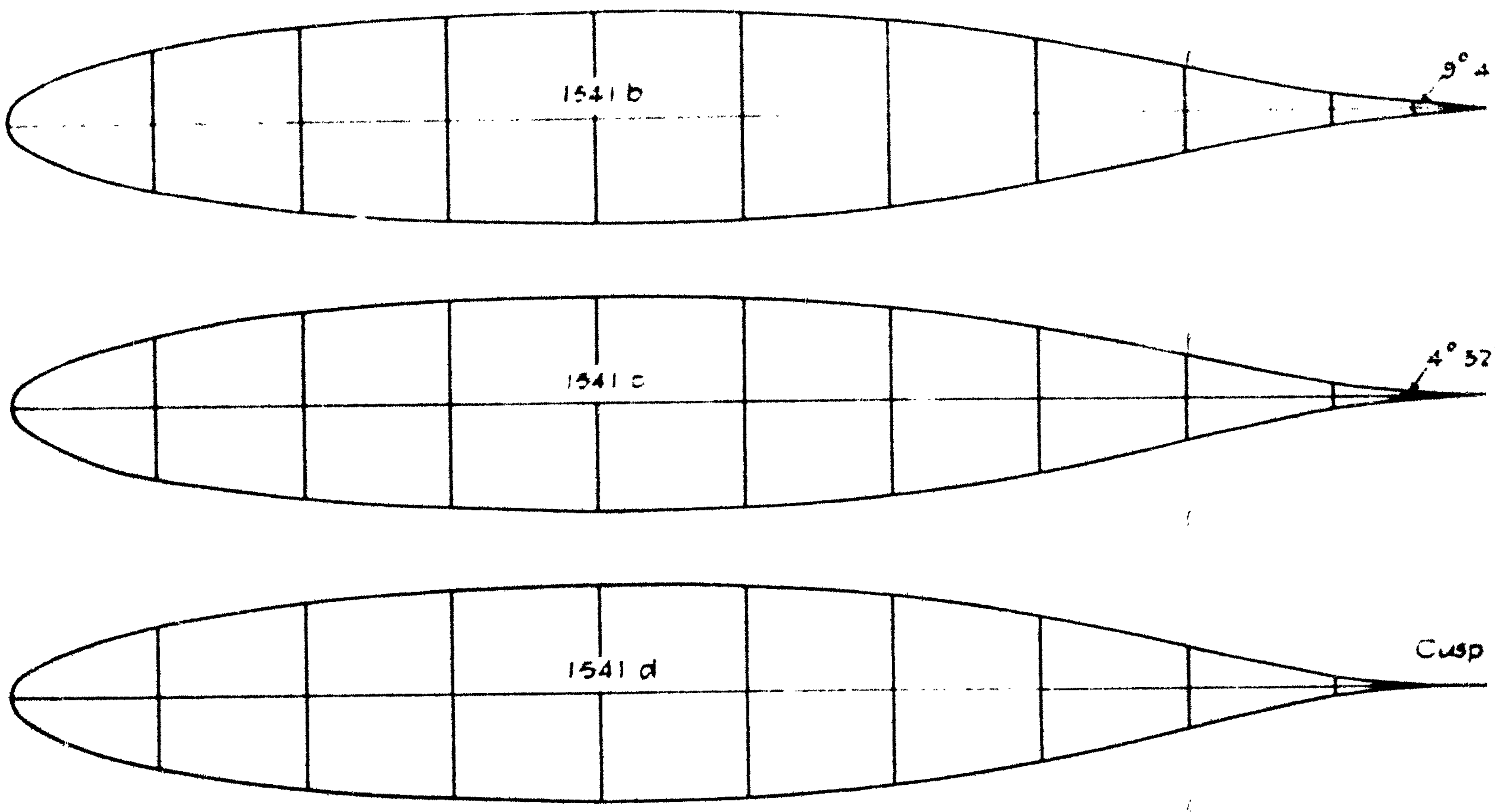

13,039
G 3

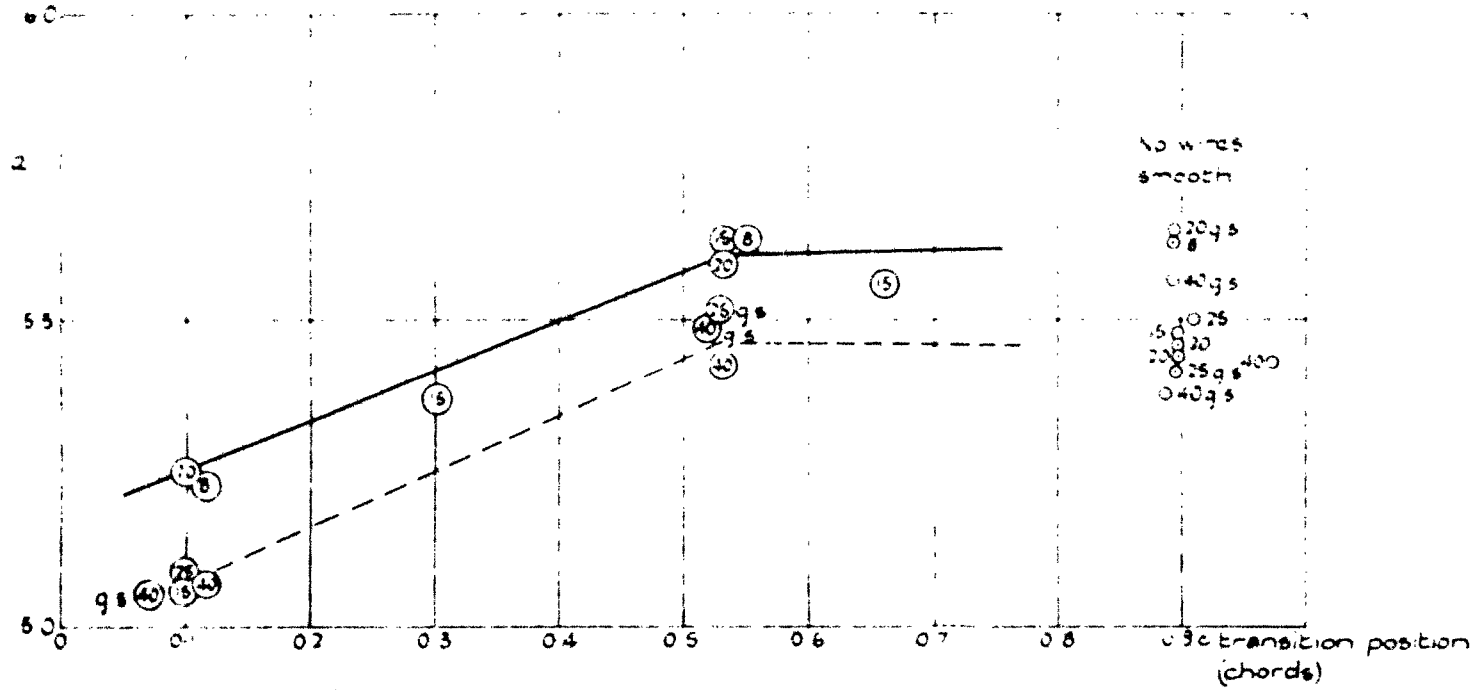

(20) means model with 20% flap set at 0°
g.s. = hinge gap grease - sealed

The Full line gives the estimated a_1 for the surfaces free from boundary layer separation. Results for no wires are plotted to the scale of a_1 but not on the scale of transition

Lift slope of 1541a section from different models.

A.R.C. 13,039
Fig. 4.

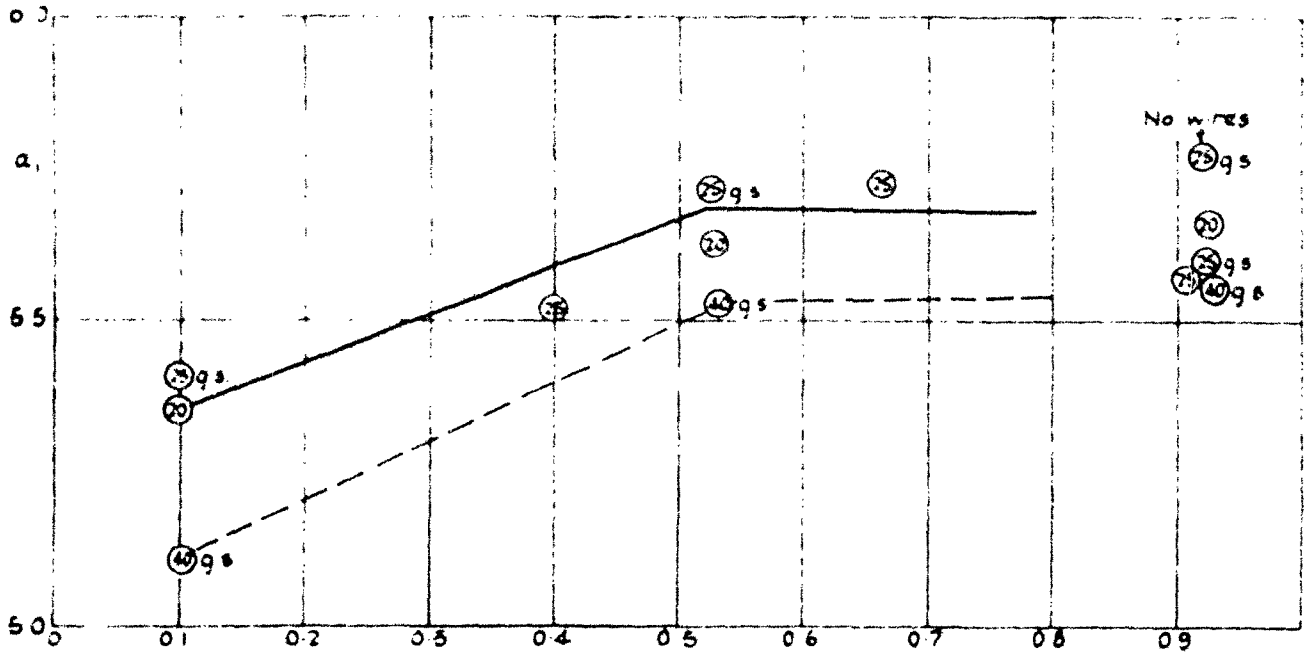

(20) means model with 20% flap set at 0°
q.s. = hinge gap grease sealed

The Full line gives the estimated a_1 for the surfaces free from boundary layer separation.
Results for no wires are plotted to the scale of a_1 but not on the scale of transition

Lift slope of 1541 section from different models.

13,039.
FIG. 5

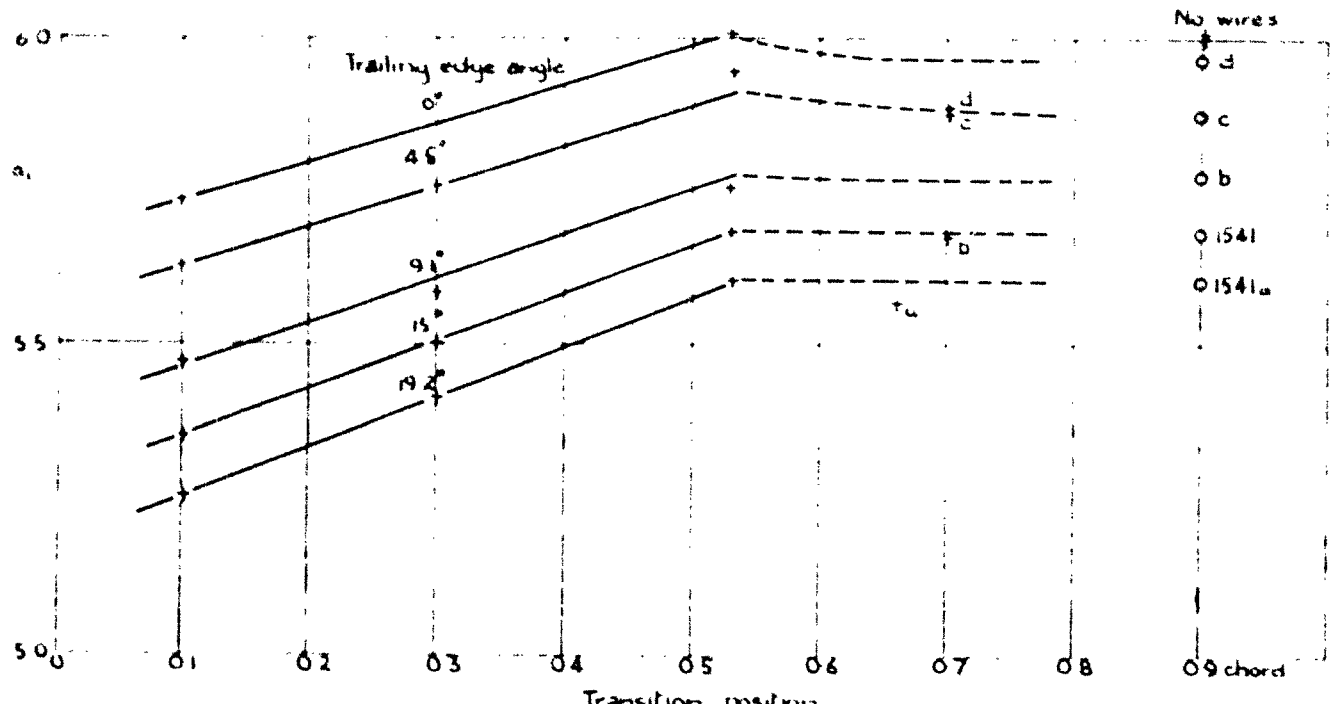

Lift Slope and Position of Transition

R.&M. 3039
Fig. 6

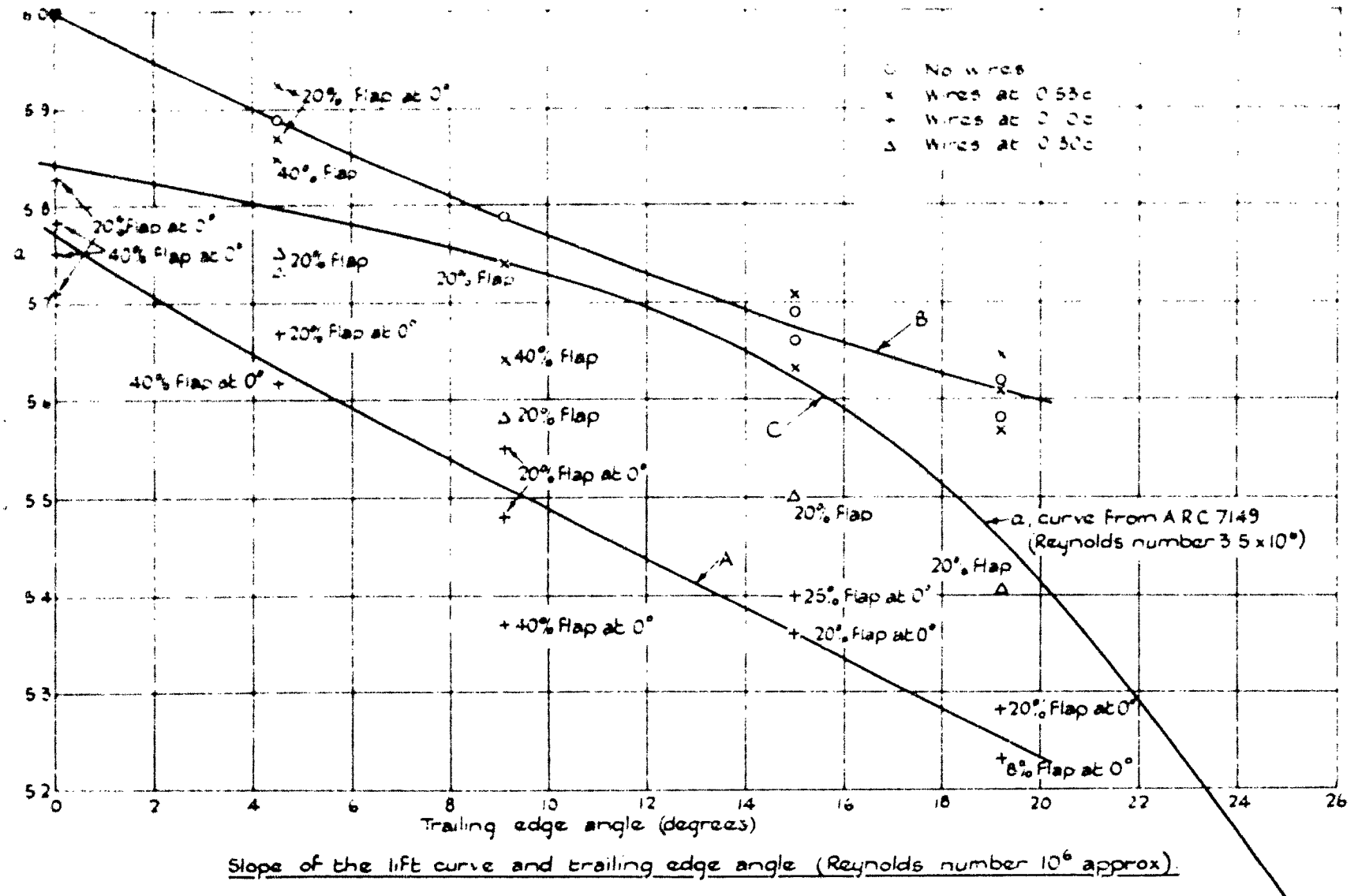

Slope of the lift curve and trailing edge angle (Reynolds number 10^6 approx).

13,039
FIG 7

FIG 8.

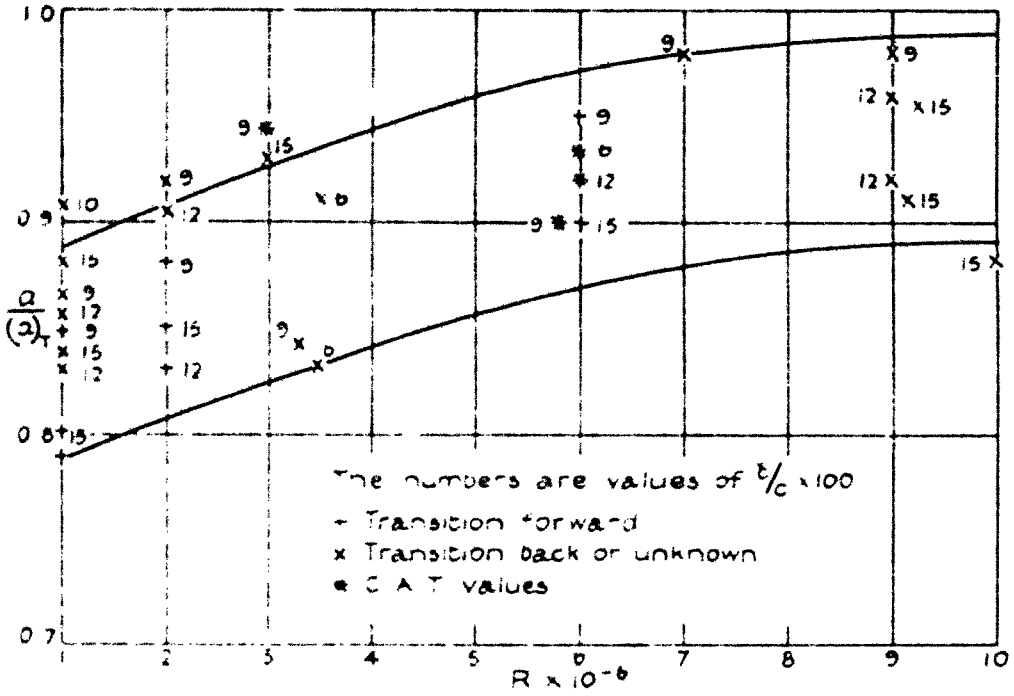

Trailing Edge Angle = 5°

FIG 9.

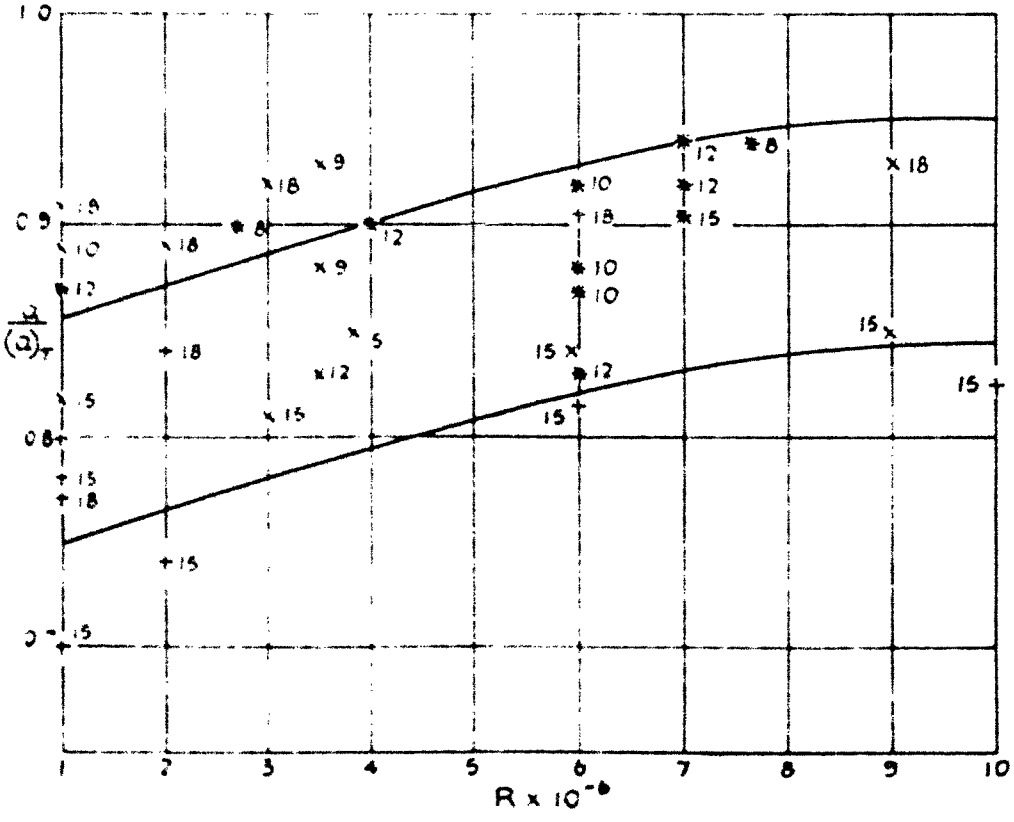

Trailing Edge Angle = 10°

FIG. 10.

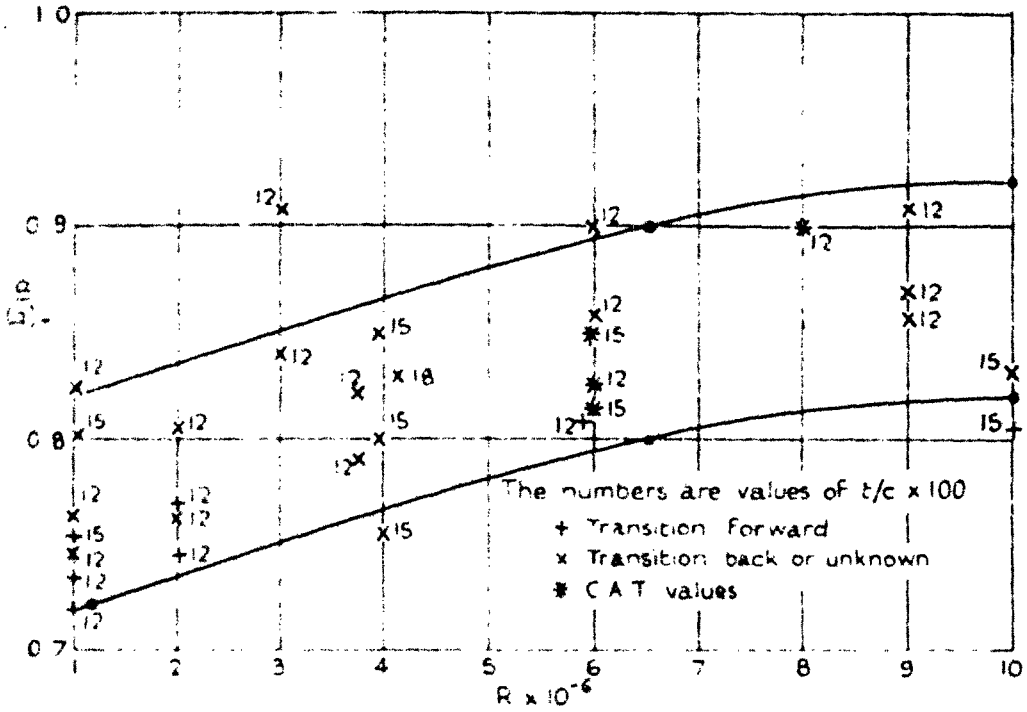

Trailing Edge Angle ≈ 15°.

FIG 11.

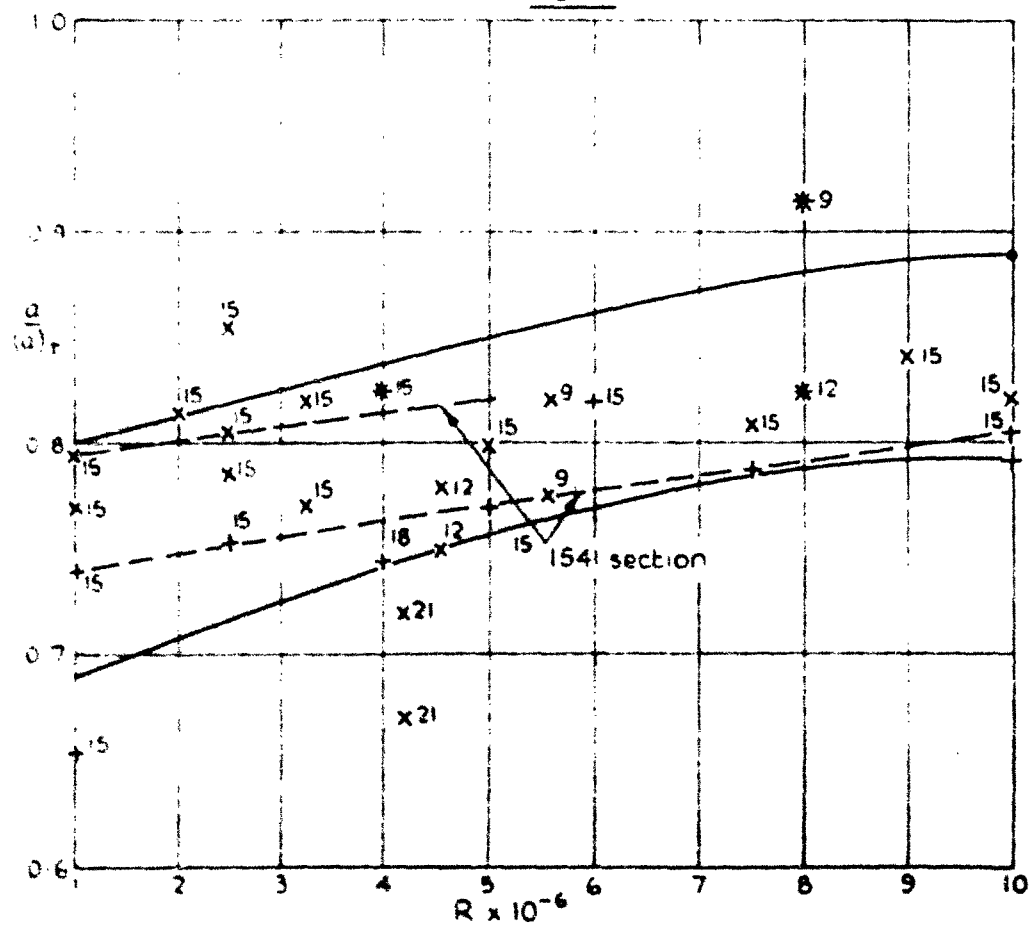

Trailing Edge Angle ≈ 20°.

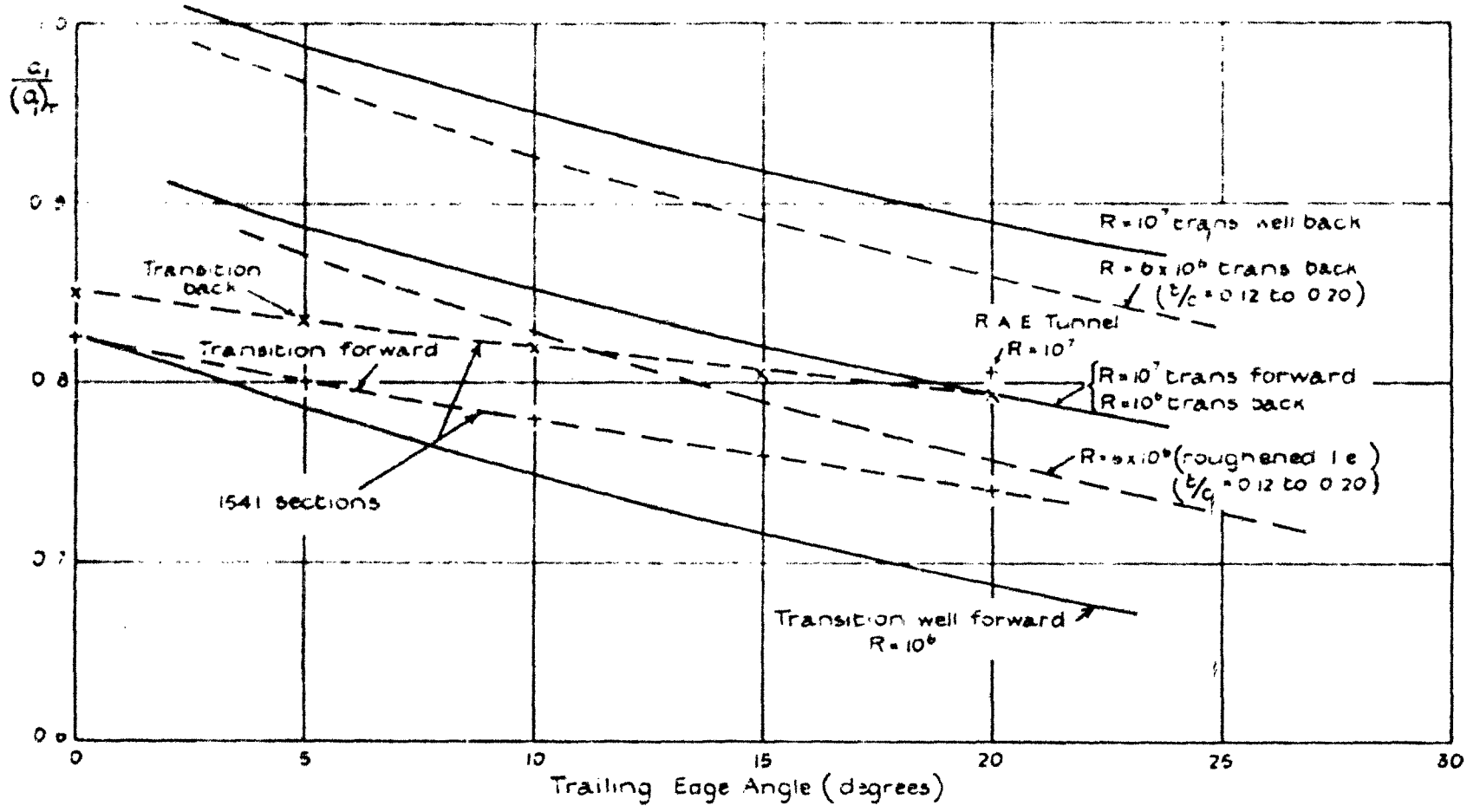

Variation of $a_1/(a_1)_T$ with Trailing Edge Angle

13,059.
FIG 12

Part II.- The Variation of Lift Coefficient with Flap Angle.

5.1. Theoretical values of the lift derivative. $\partial C_l/\partial \eta$ or a_2

To a first approximation the ratio of the theoretical values of a_2 and a_1 is independent of thickness-chord ratio, so that the curve of a_2/a_1 against flap-chord ratio, E, for a thin flat plate, given in Fig.16 may be used to determine $(a_2)_T$ from $(a_1)_T$.

5.2. Experimental results for the 15.1 series.

The ratio $a_2/(a_2)_T$ is plotted against trailing-edge angle in Fig.13, for flap-chord ratios, E = 0.2 and 0.4, and for two positions of transition. In Fig.14, $a_2/(a_2)_T$ is plotted against $a_1/(a_1)_T$. It is clear from Fig.14 that within the limits of experimental error (shown by the dotted lines for E = 0.2) there is a definite relationship between these quantities for a given value of E. A few points for N.A.C.A. 0015, from Refs. 11,12 are shown in the figure and appear on the whole to be consistent with those of this report.

The experimental results at the remaining values of E are given in Fig.15, where the ratio $a_2/(a_2)_T$ is plotted against E for a series of values of $a_1/(a_1)_T$. The experimental points have been modified slightly to make them correspond to the marked values of $a_1/(a_1)_T$ and are plotted to exhibit the degree of smoothing necessary to obtain a regular sequence of curves.

The curves of Figs.14 and 15 are certainly independent of transition position and should be independent of Reynolds number.

5.3. Chart for finding a_2/a_1

When $a_1/(a_1)_T$ has been determined, from data such as those of Fig.12, a_2/a_1 can be found from Fig.16, where it is plotted against E in a family of curves with constant $a_1/(a_1)_T$.

In Ref.4 Naylor and Lyons deduced two-dimensional values of a_2/a_1 from a large collection of data, mainly from American sources. Their two extreme curves for trailing-edge angles of 7½ degrees and 25 degrees respectively are reproduced in Fig.17, where they are shown dotted. The nearest corresponding curves from the data of this report are shown by the full lines for $a_1/(a_1)_T$ = 0.85 and 0.70 respectively. These two values of $a_1/(a_1)_T$ correspond to various combinations of the three parameters, Reynolds number, transition point, trailing-edge angle; typical sets of these quantities are shown on the figure. It is clear that all the relevant parameters must be considered when estimating lift and that Fig.3 of Ref.4 is not generalised enough for correctly estimating a_2/a_1. But the data used by Naylor and Lyons would appear to confirm that the results of the investigation of the present report, expressed in terms of the ratio $a_1/(a_1)_T$, may be confidently used over a wide range of Reynolds numbers.

Part III./

13.039
FIG. 13.

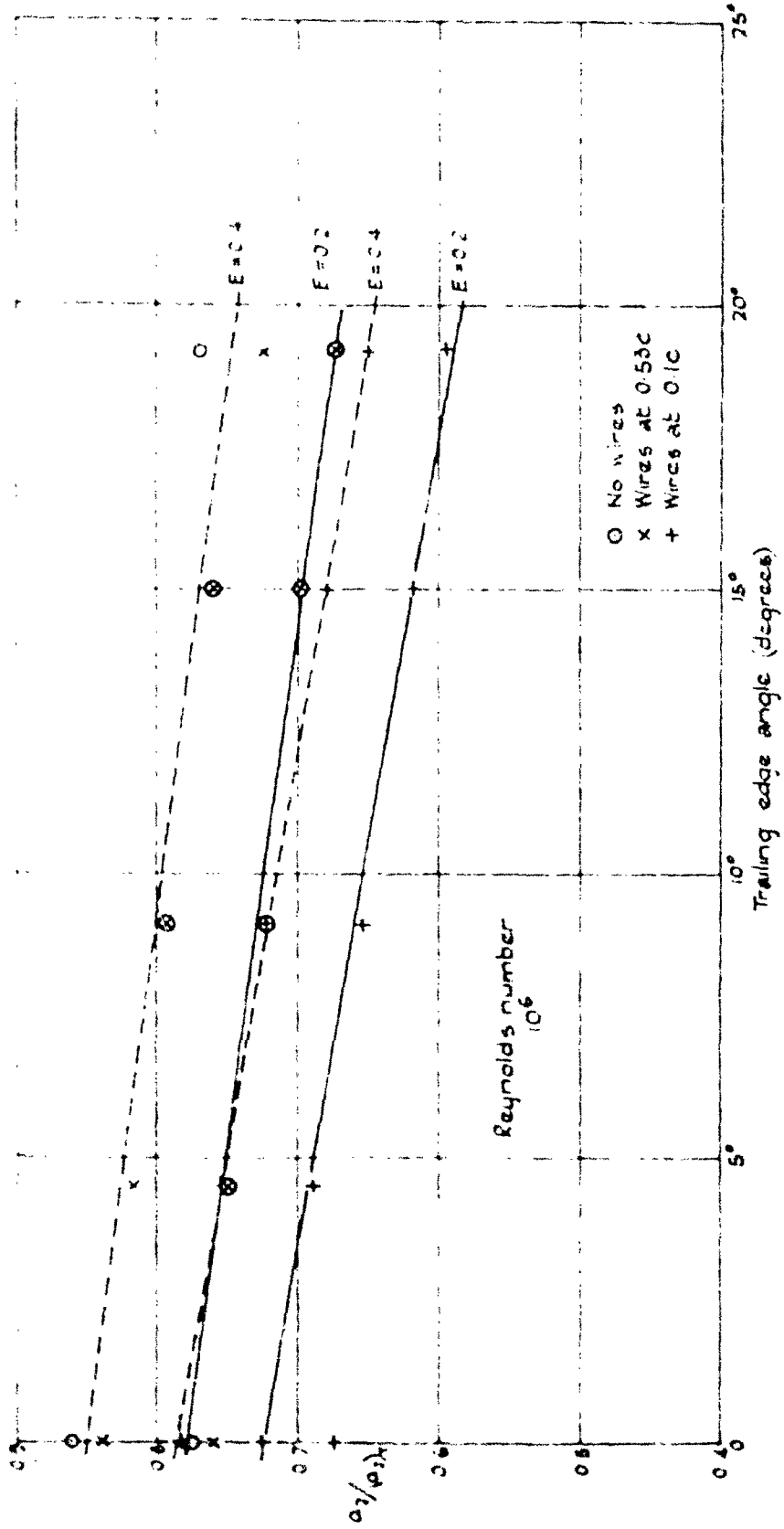
E=0.4
E=0.3
E=0.2
O No wires
× Wires at 0.53c
+ Wires at 0.1c
Reynolds number
10^6
Trailing edge angle (degrees)
0°
5°
10°
15°
20°
25°
0.4
0.5
0.6
0.7
0.8
0.9
$c_l/(c_l)_{\alpha=0}$

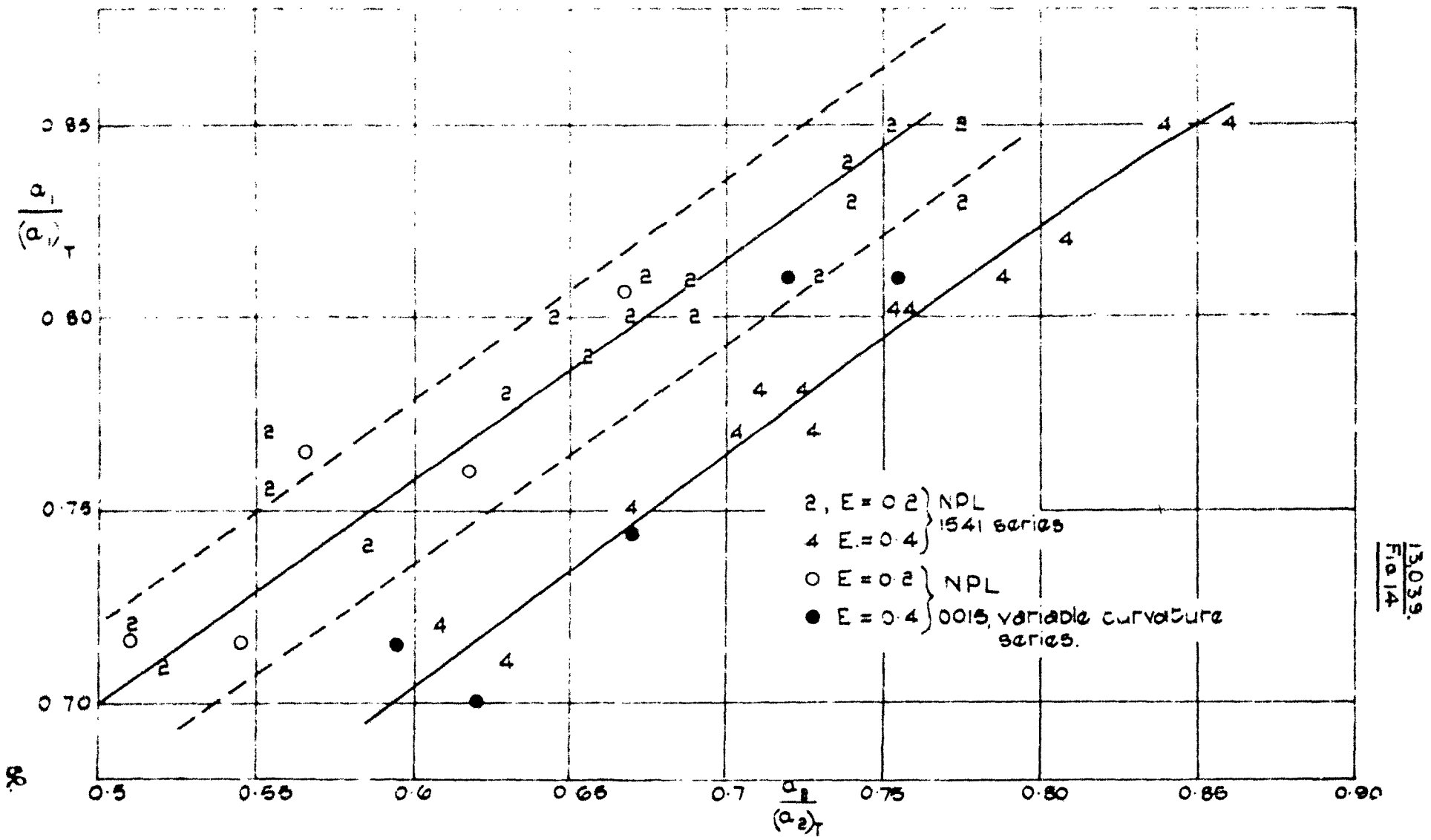
0·85
0·80
0·75
0·70
$\frac{a_1}{(a_1)_T}$
0·5
0·55
0·6
0·65
0·7
0·75
0·80
0·85
0·90
$\frac{a_2}{(a_2)_T}$
2, E = 0·2 } NPL 1541 series
4 E = 0·4 }
O E = 0·2 } NPL 0015, variable curvature series.
● E = 0·4 }

13.039.
Fig 14

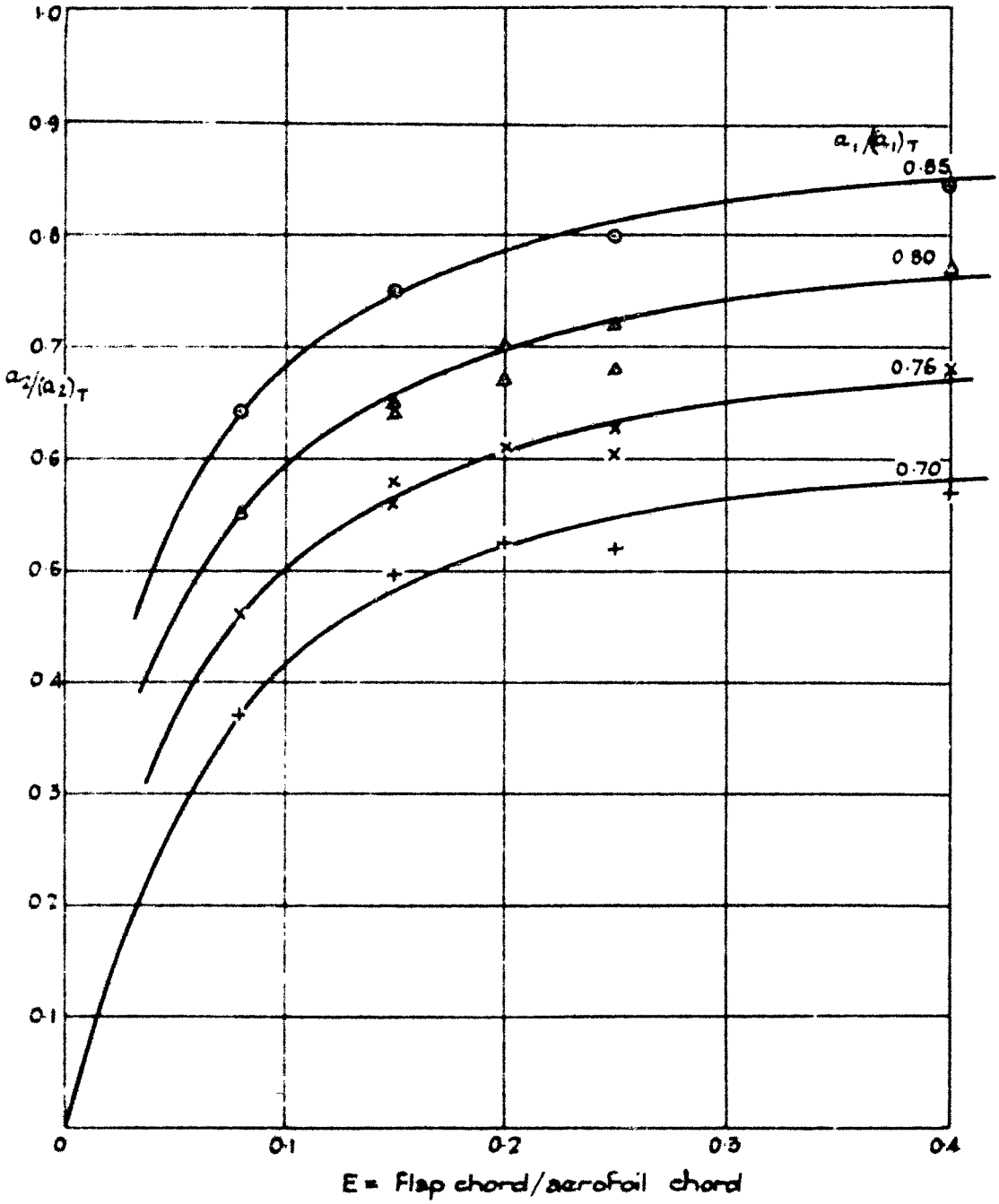

Two-dimensional Control Characteristics.

Lift due to Flap and Flap chord ratio.

R.A.E.M.

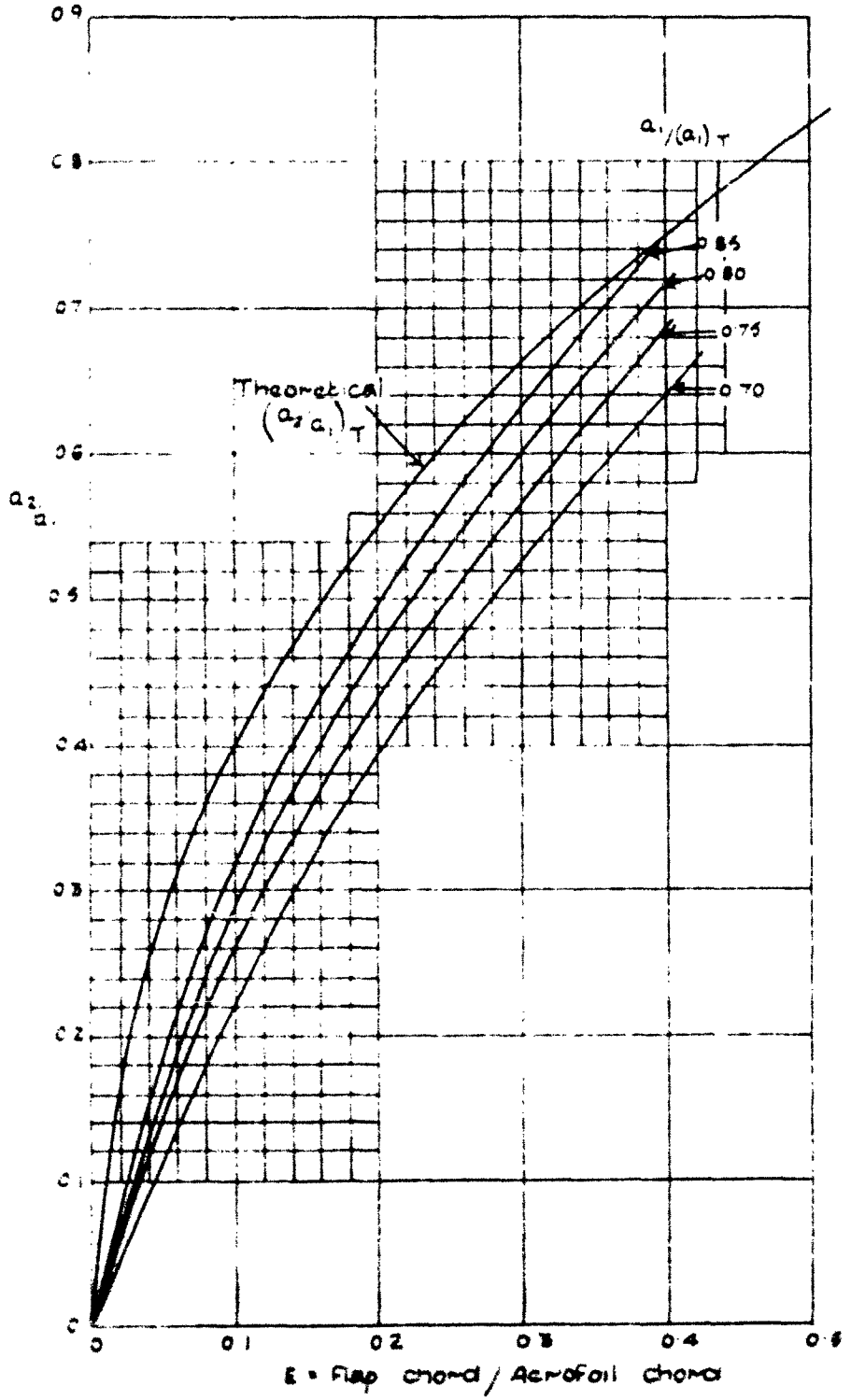

a_2/a_1 and Flap chord ratio.

E.A.S.

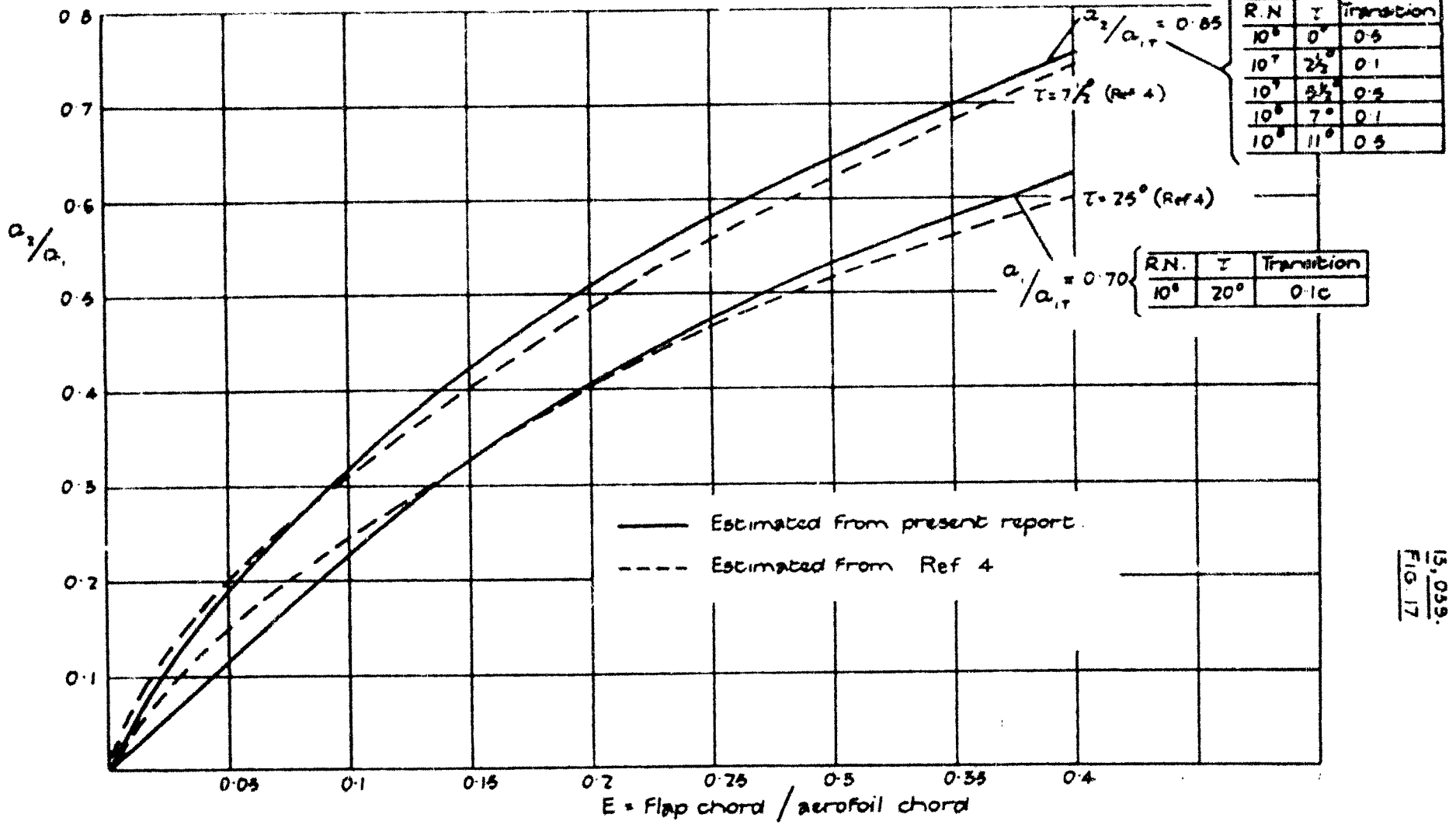
0·8
0·7
0·6
0·5
0·4
0·3
0·2
0·1
a_2/a_1
$a_2/a_{1,T} = 0·85$
$\tau = 7\frac{1}{2}°$ (Ref 4)
$\tau = 25°$ (Ref 4)
$a_1/a_{1,T} = 0·70$
R.N. | τ | Transition
10^6 | 0° | 0·5
10^7 | $2\frac{1}{2}$° | 0·1
10^7 | $5\frac{1}{2}$° | 0·5
10^6 | 7° | 0·1
10^6 | 11° | 0·5
R.N. | τ | Transition
10^6 | 20° | 0·1c
Estimated from present report
Estimated from Ref 4
0·05
0·1
0·15
0·2
0·25
0·3
0·35
0·4
E = Flap chord / aerofoil chord

13,059.
Fig. 17

Part III.- Hinge Moments on Plain Flaps.

6. Introduction.

6.1. In Ref.1 Preston at first found that a plotting of $b_1/(b_1)_T$ against $a_1/(a_1)_T$ gave an apparently unique curve for a given value of E, the flap chord/aerofoil chord ratio, but later[3] (1944) he recognised that this curve was actually only unique for a given aerofoil shape. There was still reason to believe that the curve was not dependent on Reynolds number or on the position of transition. To extend the range of experimental evidence it was decided to carry out a series of tests on new models, based on a low drag design, so that transition could be delayed beyond the half chord position. Further it was planned to modify the rear half of the model so that the trailing edge angle of the section could be reduced in stages to zero. By this means it was hoped to obtain much thinner boundary layers as well as the thicker ones characteristic of large trailing edge angles and of forward transition. This particular aim has not in fact been achieved to the extent that had been hoped and it is now realised that, apart from the possibilities of artificial reduction by suction, the boundary layer thickness can be reduced drastically only by a very large increase in the Reynolds number of test. Nevertheless, the range of trailing edge angles covered has revealed important facts about control coefficients, and has led to a possible framework for correlating a_1, a_2, b_1 and b_2 similar to that first suggested by Preston.

6.2. Description of the experiments.

The aerofoil profiles tested for the purposes outlined in the preceding paragraph are illustrated by Figs.2 and 3; they are all of thickness-chord-ratio 0.15, with maximum ordinate at 0.41c, and the series will be referred to as the 1941 series. The rear portion of the original aerofoil (called 1941, Fig.2) has been systematically modified so as to give a range of trailing edge angles from 0° to 19.2°. In the original programme, each modification was to be fitted with plain flaps with chord ratios ranging from 0.4 to 0.08, but there was time for only a portion of the programme to be completed. The transition point was varied in position from 0.1 to 0.65 of the chord from the leading edge by means of wires; in addition the transition was allowed to occur, without wires, between 0.65 and 0.70. The gap at the hinge was either extremely small, approximately 0.001, or sealed with grease in all the experiments. The Reynolds number of the tests was 0.96×10^6.

The models were 4 ft. span and 30 in. chord and were suspended from a roof lift balance by means of a parallel motion linkage outside the tunnel; they were connected to the linkage by stout steel tubes, which were surrounded between the models and the tunnel walls by dummy aerofoils of the same section as the model under test. A plan of the model and dummies as set up in the 7 ft. No.2 tunnel is given in Fig.18. The gaps between the aerofoil on the balance and the dummies at each end were of the order 1/16 in: an attempt to measure the effects of these gaps on lift and hinge moment led to the conclusion that the effects were almost within the limits of experimental error and could not be definitely determined. The effects of the gaps have therefore been treated as negligible. Hinge moments were measured by means of a wire attached to a short sting at one end of the flap and to a light balance on the roof of the tunnel. The hinges of the flap were small ball bearings, kept well cleaned and lubricated, and were practically

frictionless./

frictionless. Considerable care was taken to measure angles of incidence and flap angles accurately, because the ranges of these angles over which transition could be held fixed was small: the quantities required from the tests were slopes of lift and hinge moment with respect to these angles and could only be determined within 1 to 2, if angles could be measured to about 20.05°, and it is believed that this was in the main achieved.

List of symbols

$a_1 = \frac{\partial C_L}{\partial \alpha}$, rate of change of lift coefficient with incidence.

$a_2 = \frac{\partial C_L}{\partial \eta}$, rate of change of lift coefficient with flap setting.

$b_1 = \frac{\partial C_H}{\partial \alpha}$, rate of change of hinge moment coefficient with incidence.

$b_2 = \frac{\partial C_H}{\partial \eta}$, rate of change of hinge moment coefficient with flap setting.

t maximum thickness of wing section.

τ trailing edge angle of the section.

h height of tunnel cross section.

b breadth of tunnel cross section.

C_L' measured lift coefficient in tunnel.

C_H' measured hinge moment coefficient in tunnel.

α' measured incidence.

η' measured flap deflection.

s semi-span of model, excluding wing ends.

$\Delta\alpha$ incidence correction due to tunnel wall interference.

ΔC_L/

ΔC_L	correction of C_L due to tunnel wall interference.
ΔC_H	correction of C_H due to tunnel wall interference.
lo	distance of centre of pressure from the leading edge.
l_1	value of l for lift due to incidence change.
l_2	value of l for lift due to flap angle.
E	ratio of flap chord to aerofoil chord.
T	suffix to denote theoretical values of the coefficients a_1, a_2, b_1, b_2 for potential flow with Joukowsky value of the circulation.

7. Tunnel Interference Correction.

The two-dimensional tunnel interference has been deduced from Ref.7 (Bryant and Garner, 1937). The first correction to be applied to the measurements takes account of the increase in wind speed due to tunnel blockage. In the notation of Ref.7, § 3.1,

$$\frac{(\Delta V)}{V} = 0.62 \frac{A'}{h^2} + 0.56 \frac{t^2}{ch}$$

where A', the sectional area of the wing, is approximately given by

$$\frac{A'}{ct} = 0.67_5,$$

the tunnel height h = 7 ft., c = 30 ins., and $\frac{t}{c} = 0.15$. Thus

$$\frac{(\Delta V)}{V} = 0.0080 + 0.0040 = 0.0120 = 1.2\%,$$

and the aerodynamic pressure $\frac{1}{2}\rho V^2$ is increased by 2.4%. The measured coefficients are therefore corrected by a factor 0.976_5.

Denote/

Denote by C'_L and C'_H the measured lift and hinge moment coefficients corrected for tunnel blockage. Then, if α' is the measured incidence, in the range of linear slopes the tunnel derivatives are defined to be

$$(a_1)' = C'_L/\alpha' ,$$

$$(b_1)' = C'_H/\alpha' .$$

Similarly if α' is set to zero and the flap is given a measured deflection η for symmetrical sections

$$(a_2)' = C'_L/\eta ,$$

$$(b_2)' = C'_H/\eta$$

The interference in addition to tunnel blockage takes the form of an incidence correction ($\Delta\alpha$), and of corrections applied to C'_L and C'_H on account of the induced curvature of flow.

$$(\Delta\alpha) = \frac{\pi}{48}\left(\frac{c}{h}\right)^2 C'_L \quad (1-2l)$$

where l is the position of the centre of pressure measured as a fraction of the chord from the leading edge,

The respective corrections to C'_L, C'_H are

$$(\Delta C_L) = -\frac{\pi}{192}\left(\frac{c}{h}\right)^2 C'_L \frac{\partial C_L}{\partial\gamma} ,$$

$$(\Delta C_H) = -\frac{\pi}{192}\left(\frac{c}{h}\right)^2 C'_L \frac{\partial C_H}{\partial\gamma} ,$$

where $\dfrac{\partial C_L}{\partial\gamma} = 4\pi\dfrac{a_1}{(a_1)_T} = \dfrac{2a_1}{1+0.8\frac{c}{h}}$ approximately

and $\dfrac{\partial C_H}{\partial\gamma} = \left(\dfrac{\partial C_H}{\partial\gamma}\Big/ b_1\right)_T b_1 ,$

where/

where for plain flaps the values of $\left(\frac{\partial C_H}{\partial \gamma} \Big/ b_1\right)_T$ in Ref.7.

Table 2, with $\lambda = 0$ may be used.

It follows that the corrected experimental lift slope,

$$a_1 = \frac{C_L' + (\Delta C_L)}{a' + (\Delta a)} = \frac{1 - \frac{x}{192}\left(\frac{c}{h}\right)^2 \frac{\partial C_L}{\partial \gamma}}{\frac{1}{(a_1)} + \frac{x}{48}\left(\frac{c}{h}\right)^2 (1-2t_1)}$$

and the corrected experimental hinge moment slope,

$$b_1 = \frac{C_H' + (\Delta C_H)}{a' + (\Delta a)} = \frac{\frac{(b_1)'}{(a_1)'} - \frac{x}{192}\left(\frac{c}{h}\right)^2 \frac{\partial C_H}{\partial \gamma}}{\frac{1}{(a_1)'} + \frac{x}{48}\left(\frac{c}{h}\right)^2 (1-2t_1)},$$

where for a uniform incidence

$$t_1 = \frac{1}{4}$$

If $a' = 0$ and ξ is the measured flap deflection, the free stream conditions corresponding to the tunnel test are a uniform incidence (Δa)
a flap deflection η
and $$C_L = C_L' + (\Delta C_L)$$

$$C_H = C_H' + (\Delta C_H).$$

It is now supposed that a_1 and b_1 are independent of ξ and the small incidence is represented by respective negative corrections $-a_1(\Delta a)$, $-b_1(\Delta a)$ to C_L, C_H. Then

$$a_2 = (a_2)'\left[1 - \frac{x}{192}\left(\frac{c}{h}\right)^2 \frac{\partial C_L}{\partial \gamma} - a_1\left\{\frac{x}{48}\left(\frac{c}{h}\right)^2 (1-2t_2)\right\}\right]$$

$$b_2 = (b_2)' - (a_2)'\left[\frac{x}{192}\left(\frac{c}{h}\right)^2 \frac{\partial C_H}{\partial \gamma} + b_1\left\{\frac{x}{48}\frac{c}{h}^2 (1-2t_2)\right\}\right]$$

where t_2 depends on the flap chord ratio E and is given in Ref.7, Table 1.

The/

The corrections are finally expressed in the convenient form

$$a_1 = \frac{(a_1)'}{1 + (F+G)(a_1)'},$$

$$b_1 = \frac{(b_1)'}{1 + (G+H)(a_1)'}$$

$$a_2 = (a_2)' - (a_2)' a_1 (F + G - J),$$

$$b_2 = (b_2)' - (a_2)' b_1 (G + H - J),$$

where $$F = \frac{\pi}{192}\left(\frac{c}{h}\right)^2 \cdot \frac{2}{1 + 0.8\,\frac{t}{c}} = 0.00373,$$

$$G = \frac{\pi}{48}\left(\frac{c}{h}\right)^2 \cdot \frac{1}{2} = 0.00197,$$

$$H = \frac{\pi}{48}\left(\frac{c}{h}\right)^2 \left(\frac{\partial C_H}{\partial \gamma}\Big/ b_1\right)_T = 0.002087 \left(\frac{\partial C_H}{\partial \gamma}\Big/ b_1\right)_T,$$

where $\left(\frac{\partial C_H}{\partial \gamma}\Big/ b_1\right)_T$ is given in Ref.5, Table 2,

$$J = \frac{\pi}{24}\left(\frac{c}{h}\right)^2 (l_2 - \tfrac{1}{4}) = 0.01670\ (l_2 - \tfrac{1}{4}),$$

where l_2 is given in Ref.5, Table 1.

8. Results of the determination of $b_1(\partial C_H/\partial \alpha)$.

In Fig.19 are given the results of special computations of $(b_1)_T$ divided by $(a_1)_T$, for the 1541 series and for Piercy sections of different t/c and τ. It will be noted that the theoretical value of b_1/a_1 is a function mainly of E and t/c, and to a minor degree of trailing-edge angle, τ. To facilitate interpolation Fig.19a is included, where $(b_1/a_1)_T$ is plotted against E for τ = 10 deg., and for evenly spaced values of t/c. The curve for zero thickness is of course that for a thin plate (Ref. 8). The inset figure in Fig.19a provides for the correction necessary if τ is not 10 deg. for the section under

consideration/

consideration. If the maximum thickness of the section occurs further forward than about 0.35c it is preferable to use the method given by Thomas in Ref.13 for the estimation of $(b_1)_T$.

The experimental values of b_1 are collected and exhibited in Figs.20, 21 and 22. In Fig.20 $b_1/(b_1)_T$ is plotted against E. It will be noted that the groups of curves for each trailing-edge angle are separated from one another. For medium values of τ there is little change in $b_1/(b_1)_T$ with E; for larger values of τ , $b_1/(b_1)_T$ increases with E , whilst for smaller values of τ , $b_1/(b_1)_T$ decreases with increase of E . It is remarkable that $b_1/(b_1)_T$ can actually exceed unity by a very large margin when $\tau = 0$. In Fig.21, $b_1/(b_1)_T$ is plotted against position of transition, and it will be clear that again for medium values of τ there is little change of $b_1/(b_1)_T$. It is curious that when transition is back at 0.5c and E = 0.2 the curves come closer together than when transition is either forward or very far back.

Thirdly, in Fig.22, $b_1/(b_1)_T$ is plotted against τ and the relationship between these parameters is approximately linear.

9. Results of the [illegible] of b_2 ($\partial C_H/\partial\eta$).

The theoretical values of b_2 are exhibited in Fig.23 by plotting of (b_2/b_2) [illegible]. The [illegible] curve is taken from Ref.8, and the values [illegible] were specially computed for the 1541 series of sections. [illegible] interpolating for different values of t/c a family of curves, for τ = 10 deg., was calculated by Thomas's method, Ref.13, [illegible] given in Fig.23a. Correction curves for use when τ is not 10 deg. are inset in the figure.

In Figs.24 and 25, $b_2/(b_2)_T$ is plotted against position of transition and trailing-edge angle respectively. Here again $b_2/(b_2)_T$ varies little with transition or with E when τ has a medium value. The relation between $b_2/(b_2)_T$ and τ is not quite linear; the curves are considerably steeper for transition forward than for transition back.

10. Relation between b_1 and a_1.

10.1 The next two figures, 26 and 27, show the relationship between $b_1/(b_1)_T$ and $a_1/(a_1)_T$. On the assumption that b_1 will have its

theoretical/

theoretical value when $a_1/(a_1)_T$ is unity, the quantity plotted is $b_1/(b_1)_T$ divided by $a_1/(a_1)_T$, which should tend to unity as $a_1/(a_1)_T$ tends to unity for all aerofoils. In each figure the graphs for the 15A1 series are drawn for transitions 0.1c and 0.5c, R being approximately 10^6. Curves for each trailing-edge angle are suggested which all meet in the neighbourhood of unity for both the plotted quantities.

10.2. Fig.26 is drawn for $\bar{z} = 0.2$. From the results of the tests on the 15A1a section ($\tau = 20$ deg.) done in the R.A.E. tunnel No.2 11½ ft. by 8½ ft., the points for two transition positions are plotted along the lowest curve, to which they belong. The agreement is extraordinarily good for this class of measurement, and gives some grounds for confidence in the suggested method of generalising the results of this work.

10.3. Some further checks were sought among the numerous reports from the N.A.C.A. on this subject. Considerable difficulty was found in correlating the American work satisfactorily for this special purpose, and it was therefore concluded that a better check would be forthcoming by using curves which were recommended by American authors themselves as representative of their experimental results. Fig.13 of Ref.9 gives a family of such curves. Two values of τ, 12 deg. and 20 deg., were selected and the corresponding values of the theoretical hinge moment coefficient, $(b_1)_T$, estimated; $(b_1)_T$ could be given values between fairly narrow limits. The quantity $a_1/(a_1)_T$ could be given a range of possible values according to t/c, etc. Finally points were plotted for each trailing-edge angle which were means of the extremes of the estimated quantities. The result of this procedure in both Fig.26 and Fig.27 (which refers to $\bar{z} = 0.4$) is satisfactory as far as it goes, and proves that American data at least give rough agreement with the proposed generalised scheme. Until further experiments designed to yield all the necessary measurements, suitably co-ordinated, are undertaken, the checking over a wider range of variables is not possible.

11. Relation between b_2 and a_1.

In Figs.28 and 29 the ratio b_2/a_1 divided by $(b_2/a_1)_T$ is given similar treatment to that given to (b_1/a_1) divided by $(b_1/a_1)_T$ in Figs.26 and 27. The graphs for two transitions 0.1c and 0.5c for the 15A1 series are drawn and tentative curves drawn to meet near (1,1). Similar checks to those in Fig.26 are shown by the plotted points in Fig.28, which are derived from the tests in the R.A.E. No.2 11½ ft. by 8½ ft. tunnel. The agreement with the curve for the trailing-edge angle 20 deg. is satisfactory for measurements of this character. The R.A.E. tunnel results for b_2 were more scattered than those for b_1.

Fig./

Fig.13 of Ref.9 was used again to compare mean values of (b_2/a_1) divided by $(b_2/a_1)_\tau$ from American sources, and the points plotted for trailing-edge angles 14 deg. and 20 deg. are in very satisfactory agreement with the generalised scheme, in both the figures 28 and 29.

One point for a trailing-edge angle of 30 deg. derived from Fig.13 of Ref.9 is plotted in Fig.28, and serves as a rough guide to extrapolation to large values of τ.

12. Effect of Transition Movement on One Surface only.

It is well known that in practice transition takes place on the upper surface of a wing a little to the rear of the point of maximum suction, apart from any local feature forward of this point which may cause premature transition. Assuming the surface to be perfectly smooth and the stream to be perfectly non-turbulent, transition on an aerofoil of 15%1 type will occur at 0.65 to 0.7c on both surfaces at small angles of incidence and will travel forward very quickly, beginning at an incidence of 2½ to 3°. On the lower surface transition will either remain at 0.65 to 0.7c. or move slowly to the rear. It is important to know therefore what happens to the hinge moments on a flap when the positions of transition are not the same on upper and lower surfaces. Accordingly some experiments were made on the 15%1 aerofoils in order to study the effect of asymmetry in transition. Fig.30 shows the results of measurement of C_{H_β} made on all five of the aerofoils at 0° incidence with flaps set at 0°, and a transition wire placed at various positions on one surface only. The effect is to give a negative lift if the wire is considered to be on the "upper" surface of the symmetrical aerofoils. But this negative lift is much larger when the trailing-edge angle τ is large than when τ is small. Some light is thrown on the reason for this by Fig.31, where C_{H_β} is plotted against position of wire. When τ = 19.2° C_{H_β} is positive for forward transition on the upper surface, decreasing of course to zero as the transition moves back to a position near that of the lower surface (0.65 to 0.7c.). However, when τ = 0, C_{H_β} is negative for forward transition on the upper surface; hence in this case there must be a positive lift on the flap which almost cancels the decreased lift on the forward part of the wing.

The ordinates of the curves Figs.30 and 31 give a measure of the jumps in C_L and C_{H_β} which would occur if transition suddenly moved forward with change of incidence. As far as C_{H_β} is concerned it is apparent that for τ = 0.20 the most favourable trailing-edge angle is 9 or 10°, if the change of C_{H_β} with transition is to be a minimum; this agrees with the conclusion above that b_1 is unaffected by transition change when τ = 9°.

Those/

These considerations are further illustrated by Figs.32 and 33. In Fig.32 C_H is plotted against α for 1541 with 25% flap in the upper figure, and for 1541a with 15% flap in the lower. τ has the value 15° in the first case and 19.2° in the second. Curves are plotted for no wires, wires at 0.1c. on both surfaces and on one surface only. From α = 0° to α = 2° the curve with no wires and that with upper wire only tend to be roughly parallel, and the two curves come together in the neighbourhood of α = 5° when the transition occurs naturally on the upper surface at about 0.1c. It is difficult to understand the observations in the upper diagram at +3°, which do not agree with sufficient accuracy with those at -3° to make the phenomena clear. It should be remarked that $\partial C_H/\partial\alpha$ with both wires is less negative than for no wires for the 1541 model.

Fig.33 applies to the 1541d model, τ = 0°. Here again from α = 0° to α = 2° the curve with no wires is approximately parallel to those with one wire. The curve for both wires is (in contrast to the case of τ = 19.2°, Fig.32) steeper than that for no wires. Also, as explained in the comments on Fig.31, the upper wire only curve is below the no wire curve at first; the two curves come together at α = 5°. The lower wire only curve coalesces with the two wire curve at α = 5°, but at a point lying above the meeting point of the two former curves; it appears that at 5° incidence the condition of the boundary layer on the lower surface is still appreciably affected by the presence of the wire at 0.1c. at 5° incidence so that the curves do not all coalesce at the same value of C_H.

It is clear that all tests of controls, when it is possible for transition to start far back at small incidence, should include cases where the transitions are asymmetrical (see Ref.10). It is not sufficient to confine the tests to the cases with natural transitions: some knowledge of the effects on lift and hinge moments of movements of transition, both symmetrically and asymmetrically is required, because the conditions of transition on model and full scale will in general be different.

13. Values of C_H at Higher Incidence and Larger Flap Angles.

So far only comparatively small changes of incidence and flap angle have been considered, and there has been no separation of the turbulent boundary-layer on the upper surface at the trailing edge. Some data are available from tests up to 10° incidence and flap angle on the aerofoils 1541 and 1541a. These data are summarised in this paragraph. Fig.34 gives two examples of the measurements of C_H for the 1541 aerofoil with trailing-edge angle 15°. C_H is plotted against $\alpha + \tau$, so that it is easy to draw curves of C_H, τ for constant α (full lines) and C_H, α for constant τ (dotted lines). The former curves are linear over the range ±5° at least so long as α lies between ±2°, whilst the latter are linear over the range ±2° so long as $|\tau| \leq 5°$. These angle ranges define the limits for which the transition points on the two surfaces can be held fixed. Outside these ranges the movements of transition and the beginnings of turbulent boundary layer separation at the trailing edge produce non-linear curves.

Fig./

Fig.35 gives examples of the effects of transition movements in the case of 15% section with trailing-edge angle 19.2°. Linearity extends over the range ±5° for the C_{H},η curves so long as $|\alpha| \leq 1°$, and over the range ±2° for the C_{H},α curves so long as $|\eta| \leq 3°$. The waves nearest the origin in the C_{H},α curves are due to the movement of transition forward in the neighbourhood of $|\alpha| = 2°$; the second turning point at about $|\alpha| = 6°$ are due to the beginnings of turbulent separation.

In the experiments illustrated by Figs.34 and 35 there were no wires to fix transition. A comparison of Fig.35 with Fig.36 where wires caused transition at 0.1c. shows that the waves in the C_{H},α curves near the origin disappear when transition is held fixed at 0.1c. and does not change at $\alpha = 2°$. Both $\partial C_{H}/\partial\alpha$ and $\partial C_{H}/\partial\eta$ are considerably reduced by the change to a forward position of transition, as has been recorded above in the discussion on b_1 and b_2. At the larger values of α and η the influence of the wires at first becomes small, because the natural transition, at any rate on the upper surface, is well forward. But the wires tend to cause an early turbulent separation on the upper surface, and wires on the lower surface are objectionable because in most cases on smooth wings the natural position for transition is well back where wires would produce complicated boundary layer profiles not representative of practical conditions. Wires are therefore only suitable for controlling transition for experimental purposes over small ranges of α of the order ±3°, and of η of ±10°.

14. Velocity Traverse at the Trailing Edge.

Total head and static pressure tubes were employed with some of the models to measure velocity profiles at the trailing edge. The instruments were traversed along lines from the trailing edge at right angles to the bisectors of each of the angles between the chord and the surface tangents; this was taken to be an approximation to the normals to the stream lines. The results are illustrated by Figs.37 and 41.

In Figs.37 to 39, the ratio of local velocity q to stream velocity U_0 is plotted against distance from the trailing edge in terms of the aerofoil chord. The approximate location of the boundary layer edge is also shown in every case.

Fig.37 refers to the no lift condition with $\alpha = \eta = 0$. The upper figure is for the condition, "wires at 0.1c.", and the lower for "no wires", with transitions at 0.65 to 0.7c. There is very little variation of δ/c, the boundary-layer thickness ratio, with section shape. It is also interesting to note the greater relative reduction of displacement thickness, readily seen from the profile shapes, due to the cusping of the section, when transition is back as compared with the forward transition.

Fig./

Fig.38 illustrates the velocity profiles for $\alpha = 2°$, $\eta = 0°$, C_L being in the neighbourhood of 0.2. There is again little effect on δ/c due to section shape in the upper figure (with wires) and in the lower figure (no wires) in the case of the lower surface. However, δ/c on the upper surface tends to become appreciably smaller as τ is reduced when transition is well back, and displacement thickness is considerably reduced on both surfaces by cusping the section.

Fig.39 covers the case $\alpha = 0°$, $\eta \rightsquigarrow 3°$ giving approximately the same C_L as in the case dealt with in Fig.38. On the whole the behaviour suggests a similarity between the effects of setting over the flap and of increasing trailing edge angle at constant incidence. The shapes of the upper surface curves with wires at 0.1c. suggest a near approach to separation.

In Fig.40, δ/c is plotted against trailing edge angle for $\alpha = 2°$, $\eta = 0$, and also for $\alpha = \eta = 0$. The curves for "no wires" are drawn full; those for "wires at 0.1c." dotted. It will be noted that δ for "no wires", lower surface, is almost unchanged by the change of incidence and by change of τ. On the other hand δ for the upper surface rises as τ increases. Trailing edge angle has little effect on δ with transition forward, but the incidence effects are a decrease in δ, lower surface, and an increase on the upper surface.

Fig.41 is similar to Fig.40 with the plottings for $\alpha = 0$, $\eta \rightsquigarrow 3°$ substituted for $\alpha = 2°$, $\eta = 0°$. The remarks made above relating to Fig.40 apply to Fig.41 in the main. With no wires the rise of δ on the upper surface with τ is much more marked.

These data are recorded in this report because it is hoped later to explain the behaviour of control flaps in terms of the properties of the boundary layers. Preston's work[2] already gives some clue to the kind of correlation to be expected, but more research is required before reliable quantitative estimations become practicable.

15. Outline of Procedure in Estimating a_1, a_2, b_1 and b_2.

It is assumed that the geometrical shape of the section, flap chord ratio, transition points, Reynolds number are known, and that an estimate of the effective trailing edge angle, τ, can be made. The value of τ should be determined from the shape of the section from 0.975c. to 1c. Then the procedure is as follows:

(1) Find $(a_1)_T$ from Fig.5, using known values of t/c and τ; or alternatively use the formula (1)

(2) Find $a_1/(a_1)_T$ from Fig.12 or Table 1, using known values of Reynolds number, transition locations, and trailing edge angle.

(3) Find a_2/a_1 from Fig.16 from $a_1/(a_1)_T$ and Z.

(4)/

(4) Find $(b_1/a_1)_T$ and therefore $(b_1)_T$ from Fig.19a, using t/c and τ; or alternatively use the method due to Thwaites for estimating $(b_1)_T$ (Ref.1[illegible]).

(5) Find $(b_2/b_1)_T$ and therefore $(b_2)_T$ from Fig.[illegible]3 or [illegible] using t/c and τ; or alternatively use Thwaites's method for $(b_2)_T$ (Ref.[illegible]).

(6) Find $b_1/(b_1)_T$ from Figs.[illegible] and [illegible], using $a_1/(a_1)_T$, E, and τ.

(7) Find $b_2/(b_2)_T$ from Figs.[illegible] and [illegible] using $a_1/(a_1)_T$, E, and τ.

(8) Some indication of the effect of movement of transition on one surface only is given by Figs.[illegible] and 31. But more data are needed, particularly with varied values of E.

16. Acknowledgements.

The authors wish to acknowledge the assistance of several of their colleagues who carried out a long and tedious sequence of experiments in connection with this work, and special thanks are due to them for the accuracy of their observations under difficult conditions. In particular Messrs. [illegible] and [illegible] Brown contributed very largely to the work of observation and reduction.

The authors wish also to express their appreciation of the skill shown by Mr. [illegible] and the workshop staff in constructing the models, which had to be finished with very special care owing to the sensitivity of control forces to small inaccuracies in shape, particularly at the trailing edge.

References

No.	Author(s)	Title, etc.
1	Batson, A. S. Preston, J. H.	The Effect of Boundary Layer Thickness on the Normal Force Distribution of Aerofoils, with Particular Reference to Control Problems. R. & M. [illegible]. April 1[illegible].
2	Preston, J. H.	The Approximate Calculation of the Lift of Symmetrical Aerofoils taking account of the Boundary Layer, with application to Control Problems. R. & M. [illegible]. May, 1[illegible].

3./

No.	Author(s)	Title, etc.
3.	Preston, J. H. Warsap, J. H.	Investigation of the Relations between Experimental and Theoretical Two-dimensional Characteristics for Two Wing - Plain Flap Combinations involving Different Flap Conventions. ...R.C.818. Nov. 1944. (Unpublished).
4.	Naylor, C. H. Lyons, D. J.	An Analysis of the Lifting Characteristics of Aerofoils and Controls with Special Reference to Methods of Estimation for Design Use. A.R.C.7149. July, 1943.
5.	Loftin, H. L., Jr. Smith, H. ...	Aerodynamic Characteristics of 15 N....C.... Airfoil Sections at Seven Reynolds Numbers. N....C.... Technical Note 1945. Oct. 1949.
6.	Loftin, H. L., Jr. Smith, H. ...	Two-dimensional Aerodynamic Characteristics of 34 Miscellaneous Airfoil Sections. N....C.... Research Memorandum, RM No.L8L08. (N....C..../T.I.B./1928). January, 1949.
7.	Bryant, L. W. Garner, H. C.	Control Testing in Wind Tunnels. (To be issued).
8.	Glauert, H.	Theoretical Relationships for an Aerofoil with Hinged Flap. R. & M.1095. April, 1927.
9.	Toll, Thos. ...	Summary of Lateral Control Research. N...C... Technical Note 1245, March, 1947.
10.	Bryant, L. W. Batson, ... S	Experiments on the Effect of Transition on Control Characteristics, with a Note on the Use of Transition Wires. R. & M.2164. November, 1944.
11.	Batson, ... S. Warsap, J. H. Brown, T. W.	Experiments on a Leading Control with Tab fitted to N....C....0015 Aerofoil, with Especial Reference to Effect of its Section on Hinge Moment and Lift. ...R.C.6980. August, 1943.
12.	Batson, ... S. Preston, J. H. Warsap, J. H.	Experiments Giving Hinge Moments and Lift on a N....C....0015 Aerofoil Fitted with a 40% Control, with Especial Reference to Effect of Curvature of Control Surface. ...R.C.6666. April, 1943.
13.	Thomas, H. W. B. M.	Correlation of Experimental and Theoretical Hinge Moments for Plain Controls. ...R.C.11461. March, 1948.

13,039.
FIG 18

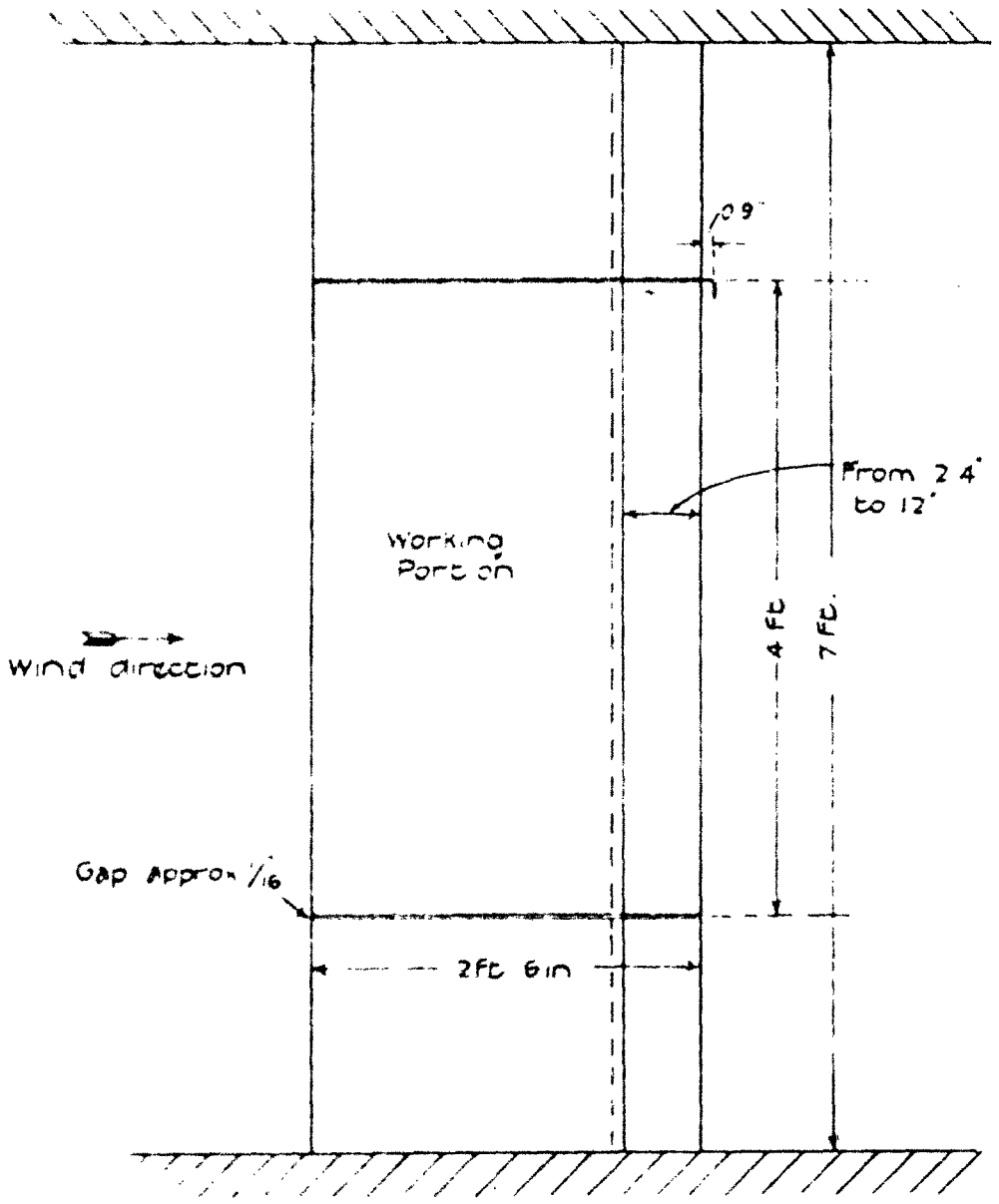
.09"
From 24"
to 12"
Working
Part on
4 Ft
7 Ft.
Wind direction
Gap Approx 1/16
2Ft 6in

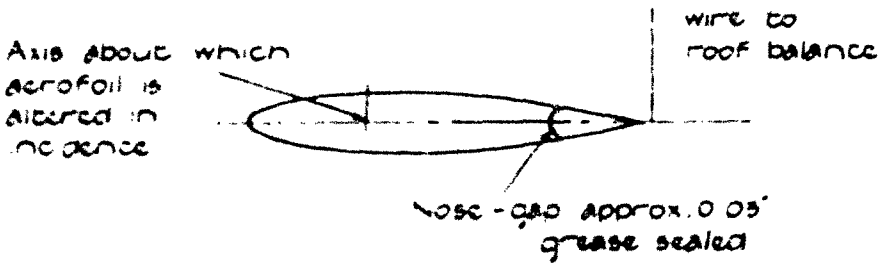
wire to
roof balance
Axis about which
aerofoil is
altered in
incidence
Nose - gap approx. 0.05"
grease sealed

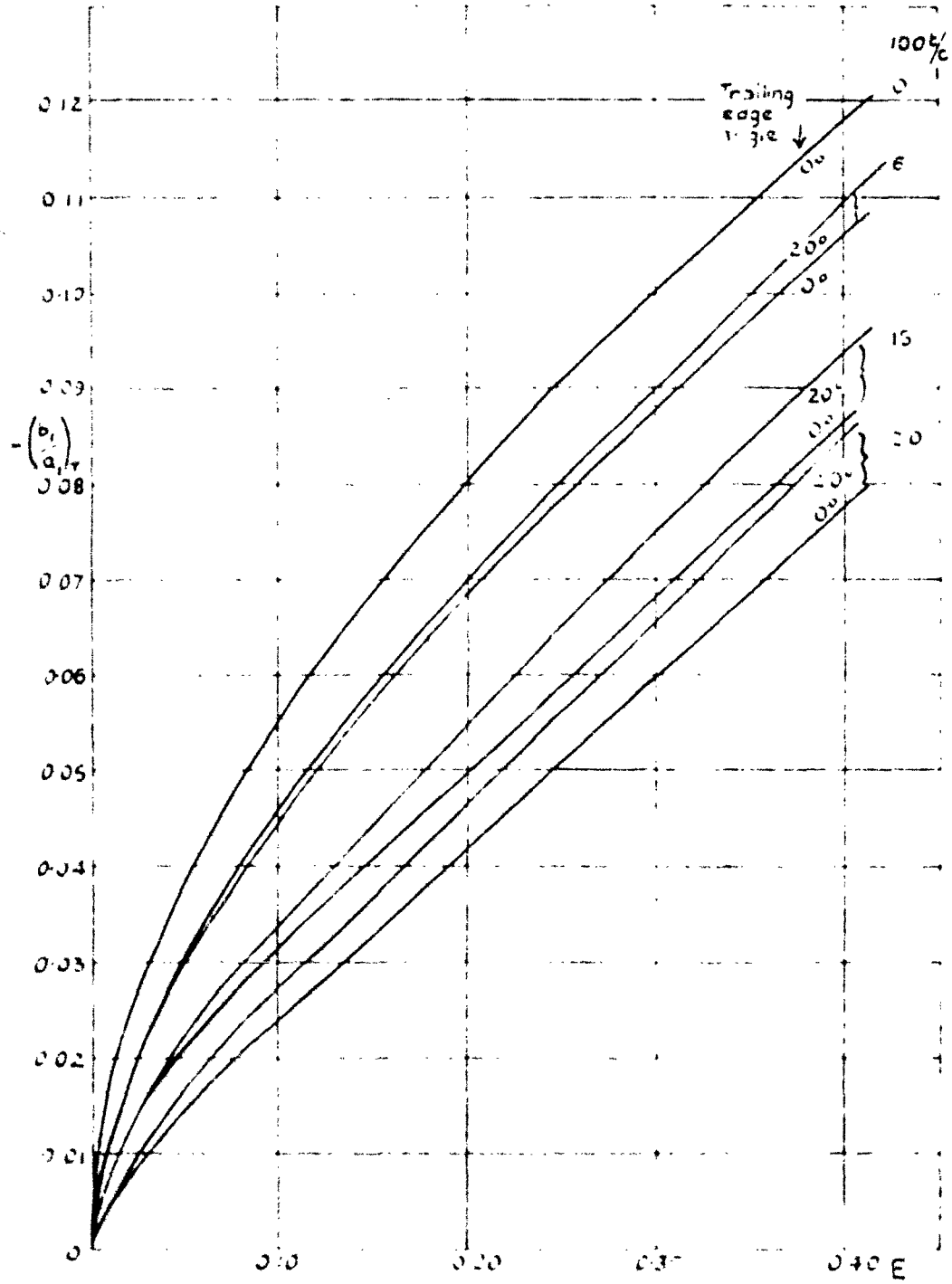

Theoretical values of $\frac{b_1}{a}$

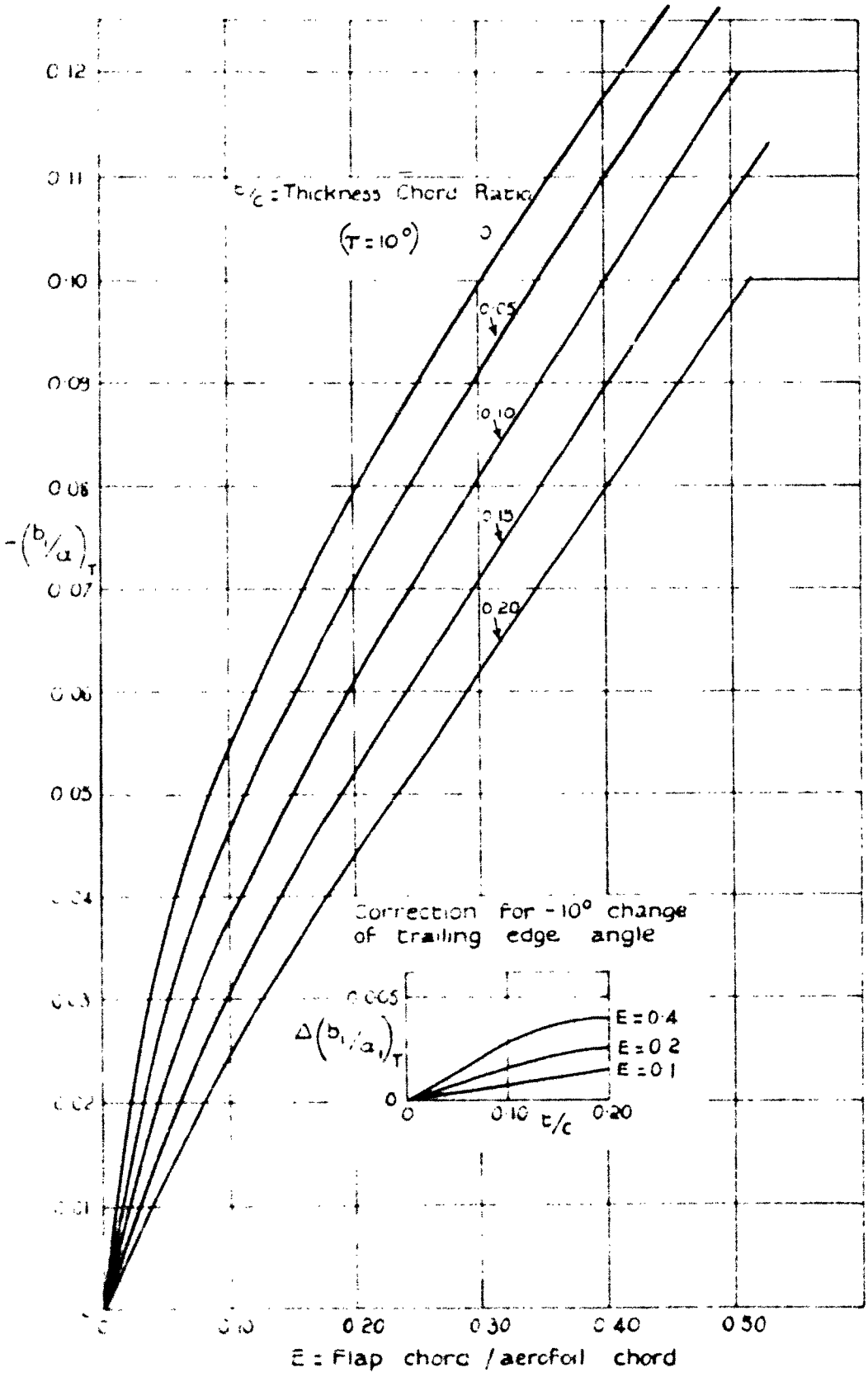

Theoretical Values of b_1/a_1

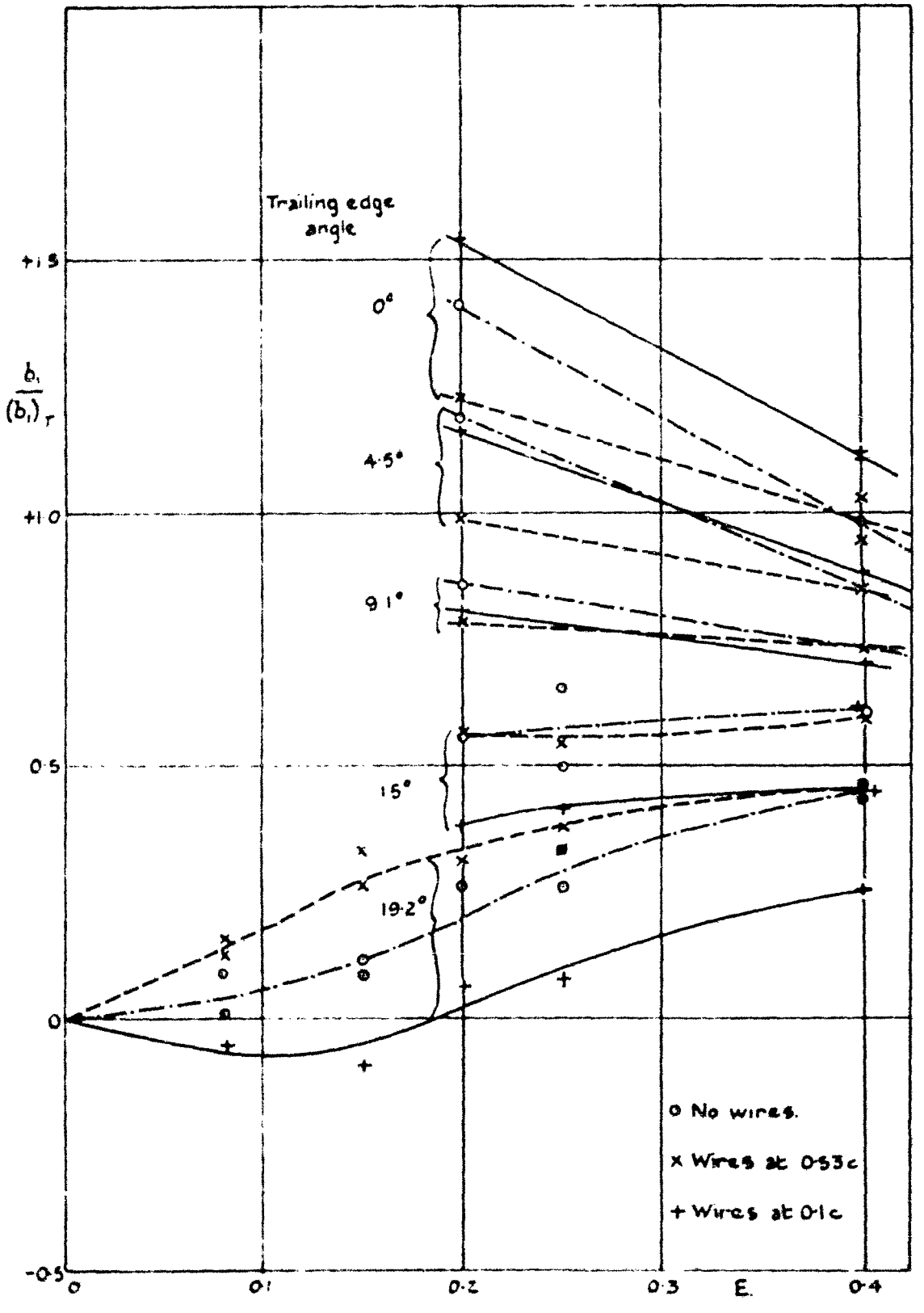

Change of hinge moment with incidence.
Effect of flap chord ratio. Reynolds number 10^6

13,039
FIG 21.

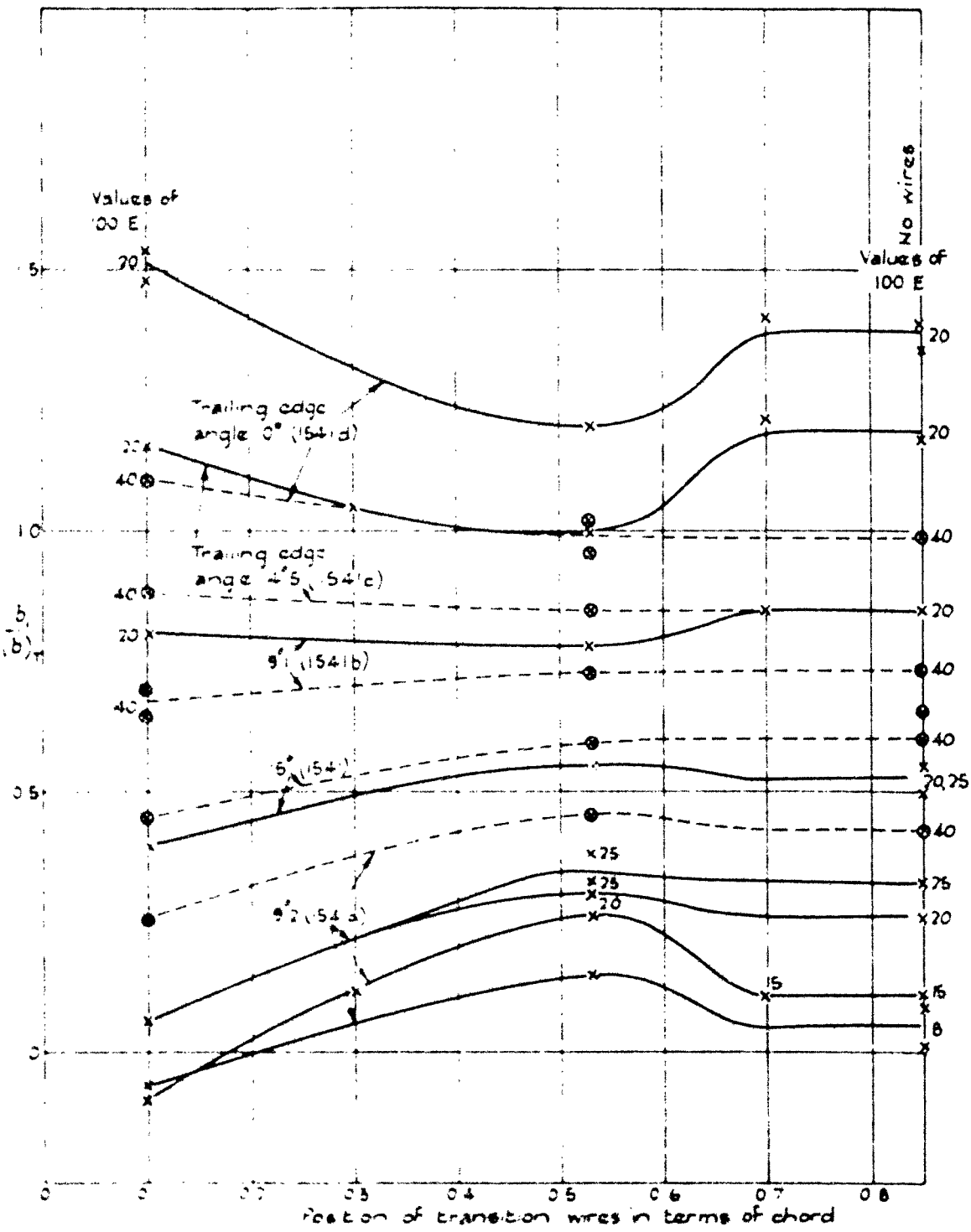

Change of range moment with incidence Effect of position of transition

Reynolds number 10^6

E.E.M.

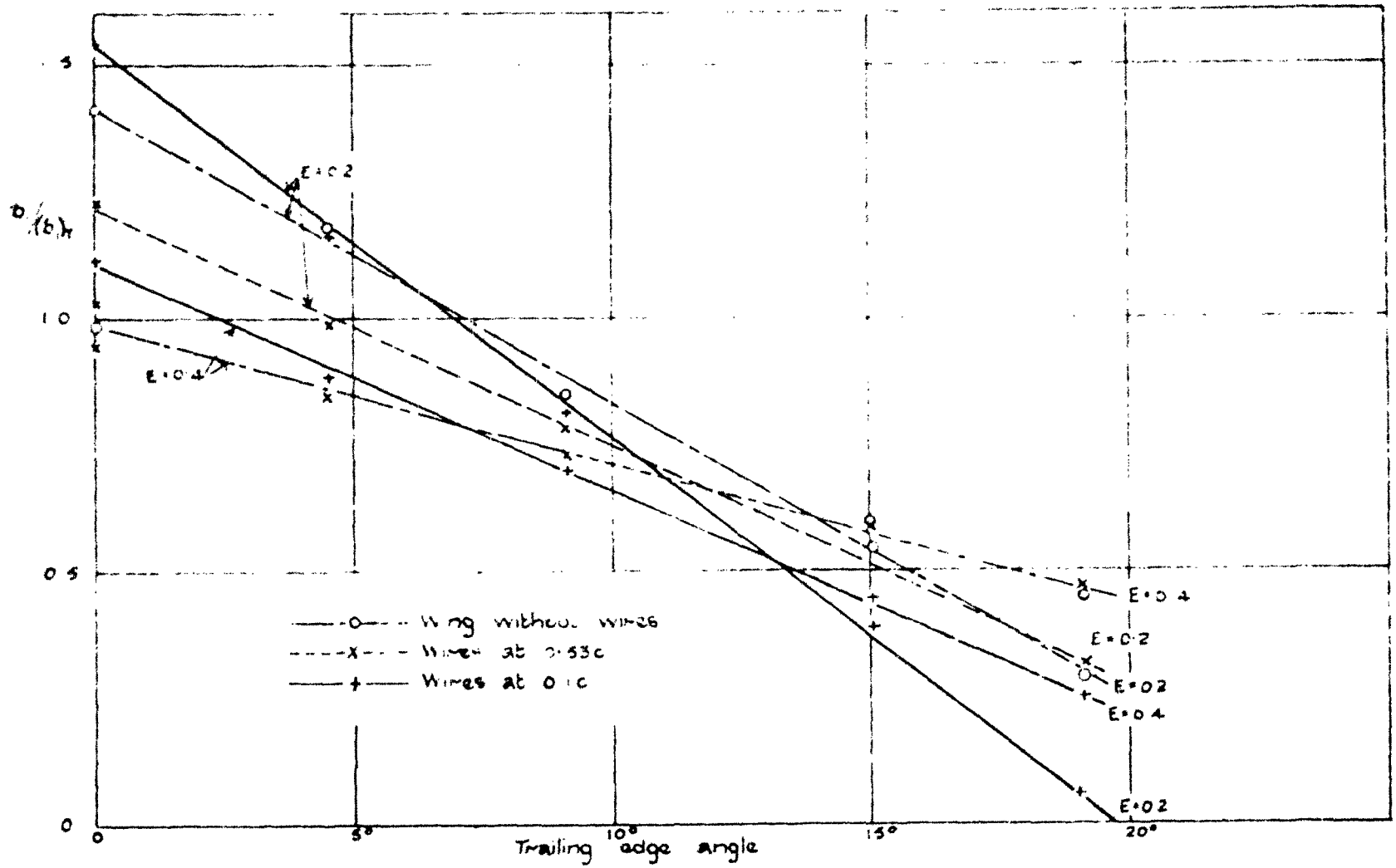

Change of hinge moment with incidence. Effect of trailing edge angle.
Reynolds number 10^6

13,039
FIG 27

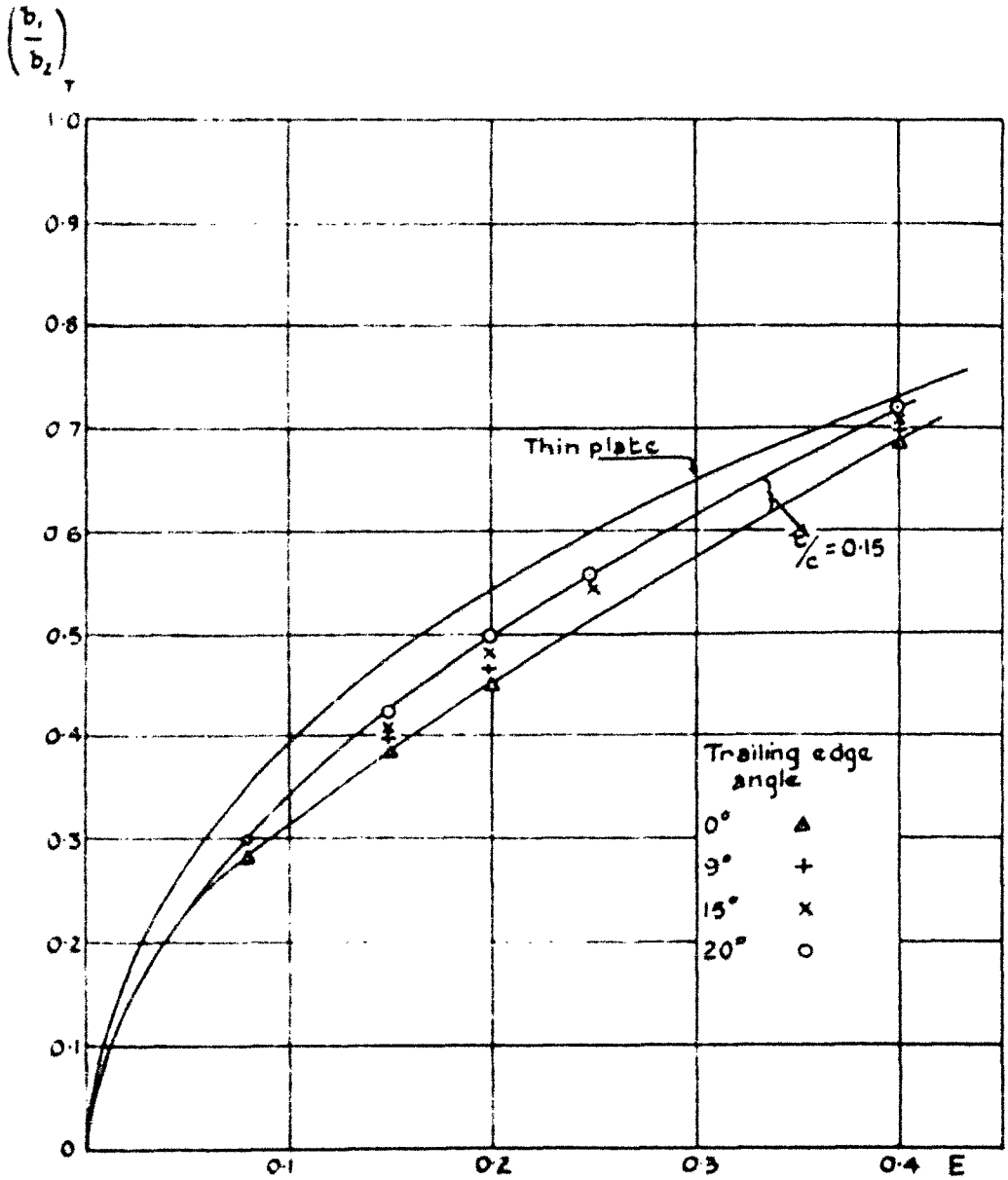

Theoretical values of $\frac{b_1}{b_2}$

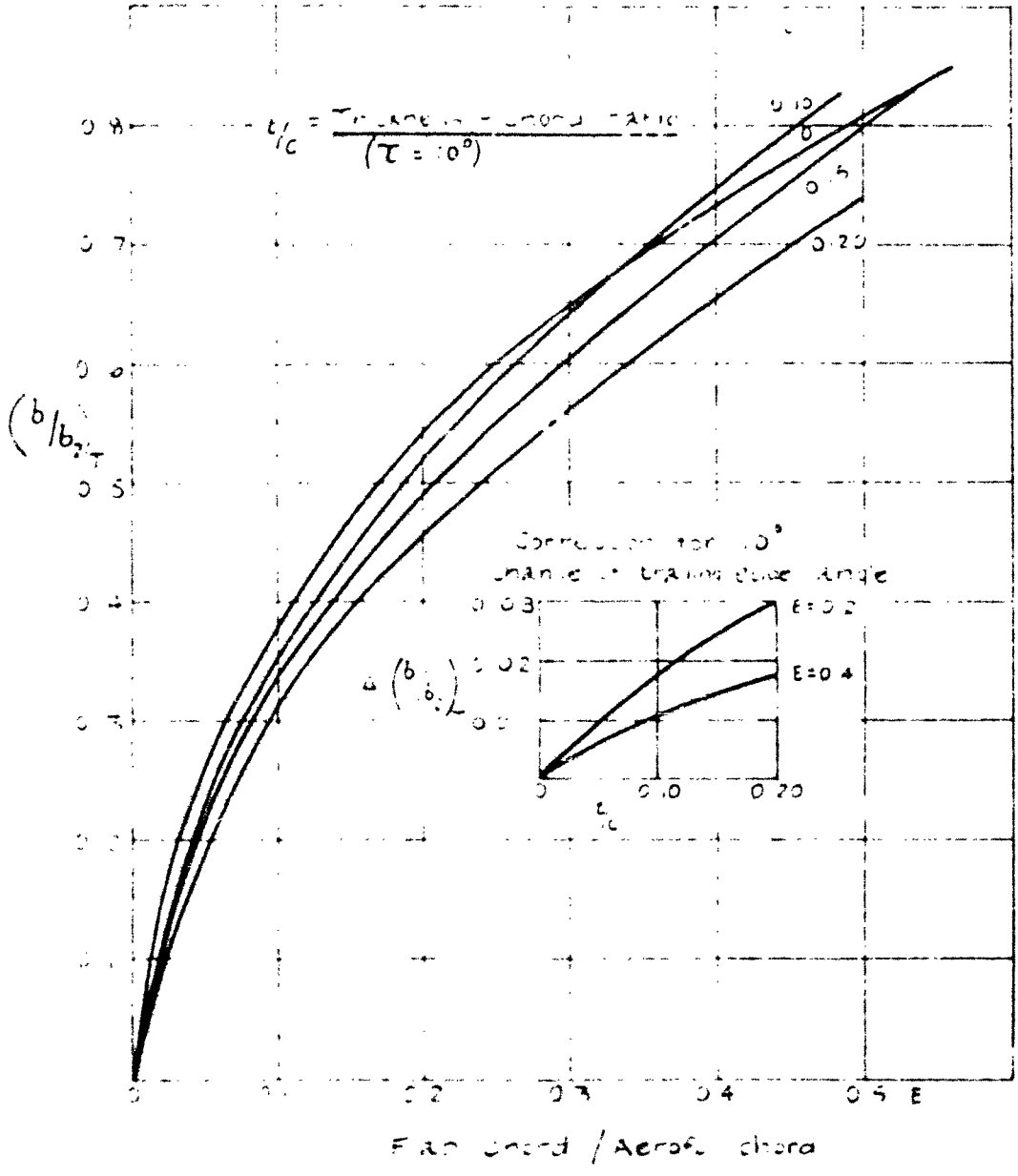

Theoretical values of b/b_2

13,039.
FIG. 24

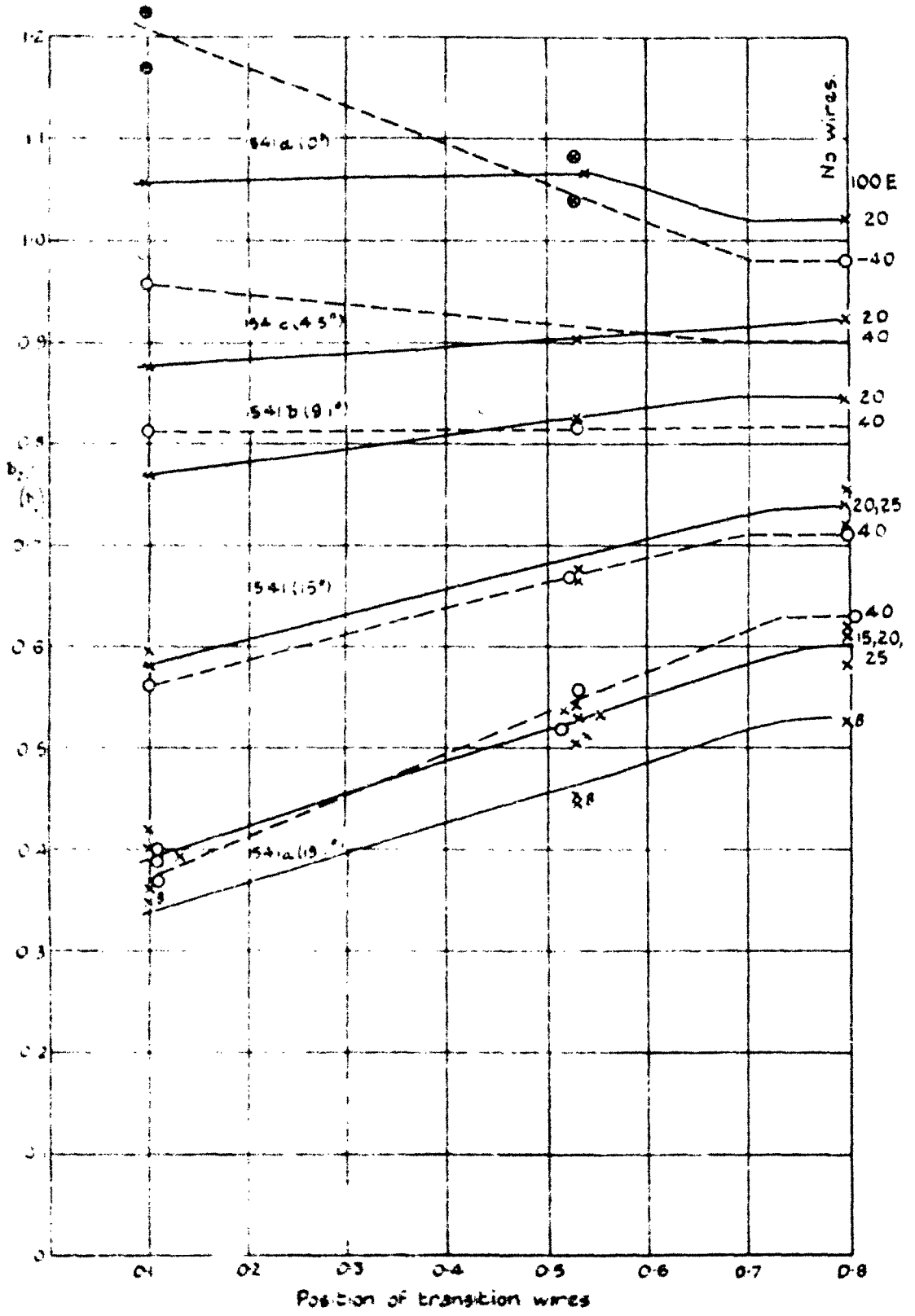

Change of hinge moment with flap angle. Effect of position of transition
Reynolds number 10^6

RM

R & M 30
FIG. 25

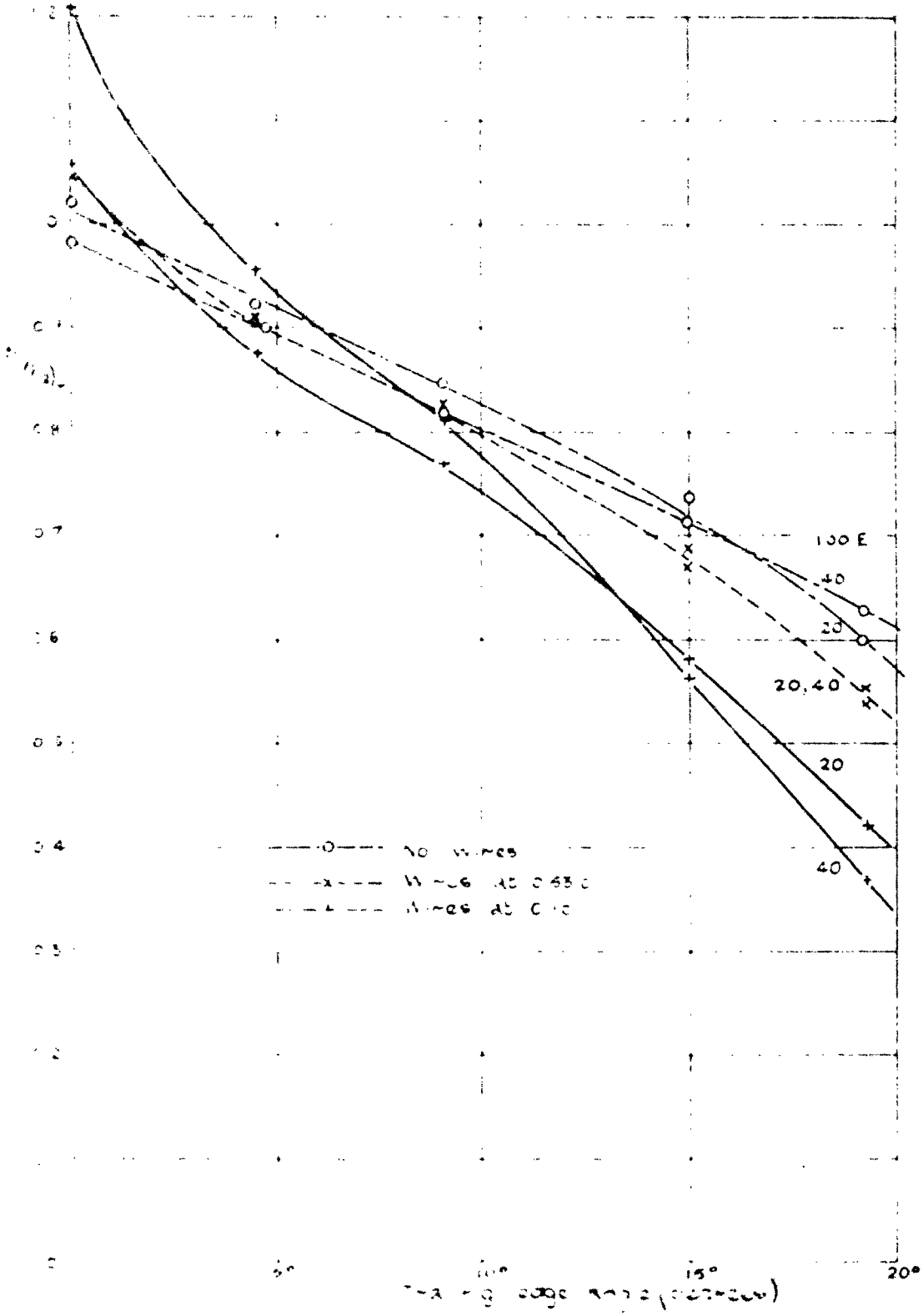

Change of edge moment with fin angle
Effect of trailing edge angle
Reynolds number 10^6

EPS

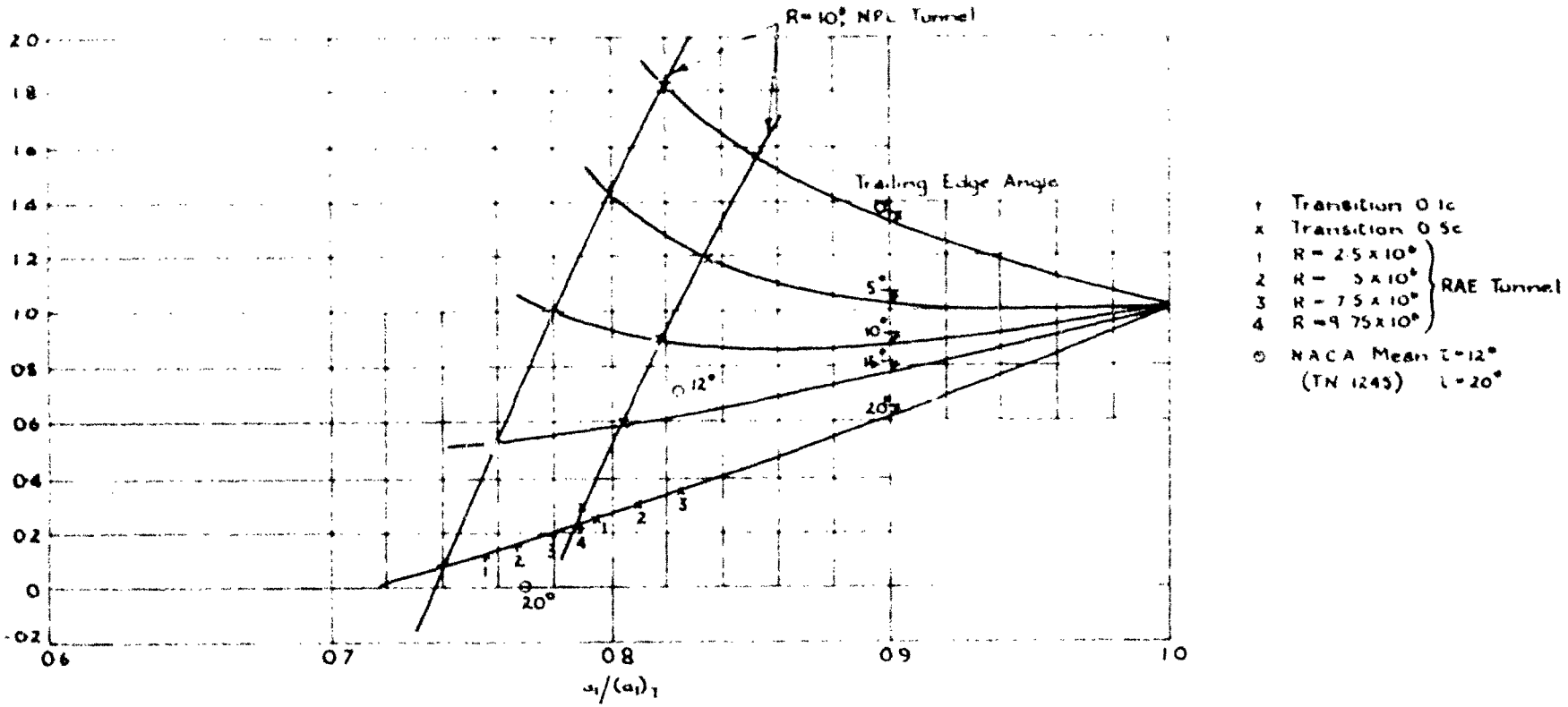

Two-Dimensional Flap Hinge-Moments E = 0·2 Chart for b_1/a_1

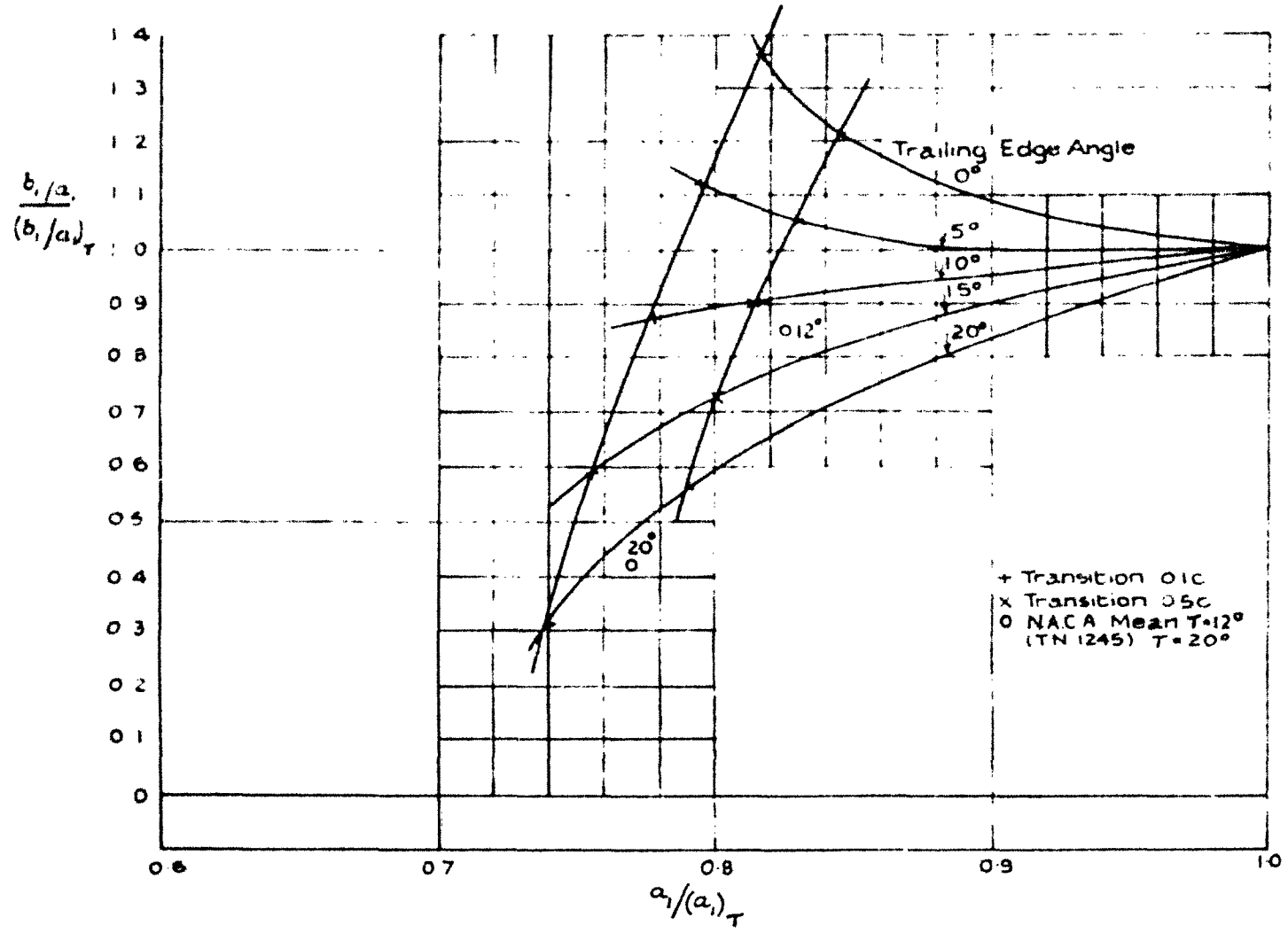

Two-dimensional Flap Hinge moments. E = 0·4 Chart for b_1/a_1.

13.039
FIG.27.

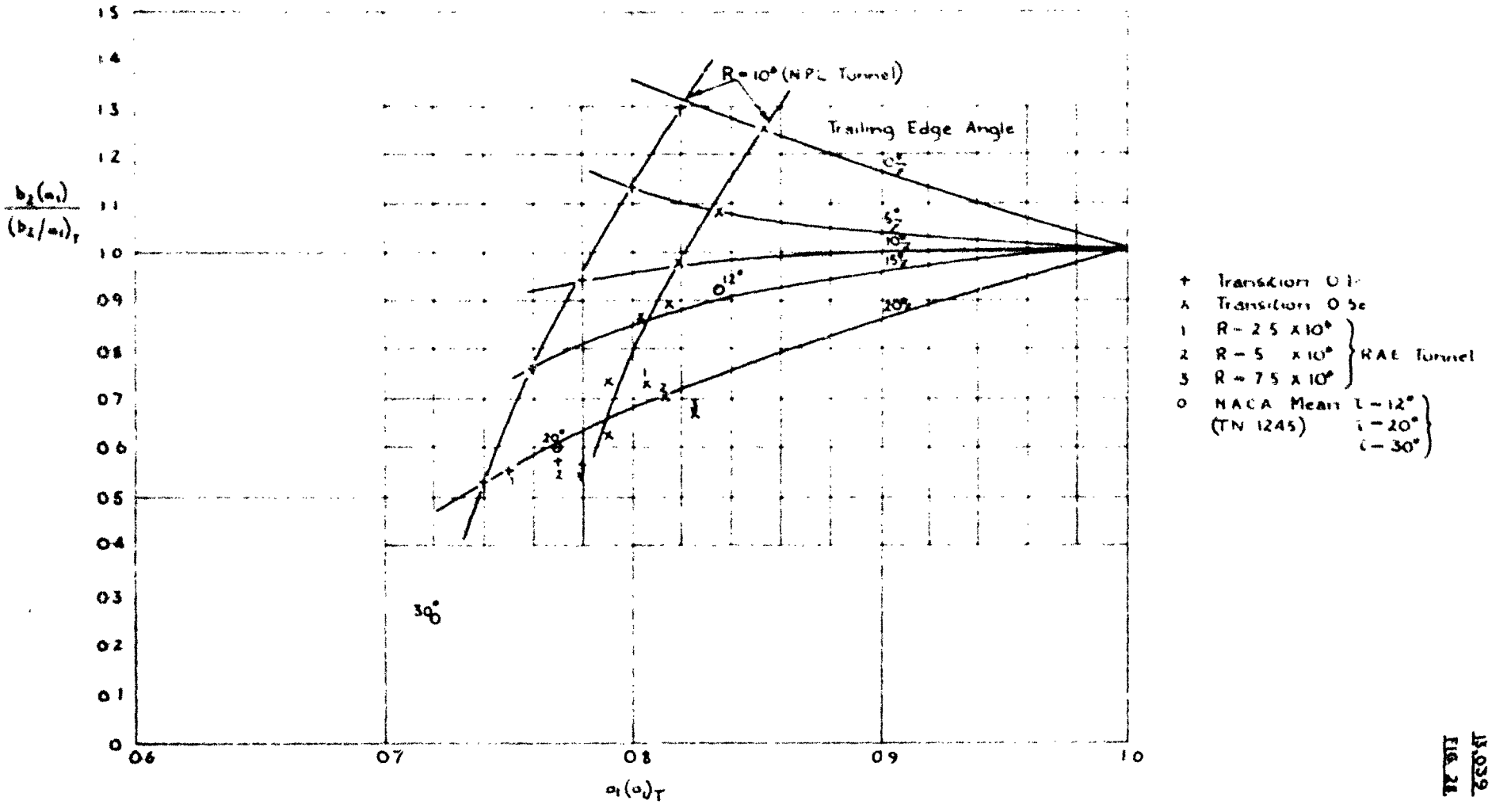

Two-Dimensional Flap Hinge-Moments E-0·2 Chart for b_2/a_1

11,039
Fig. 24

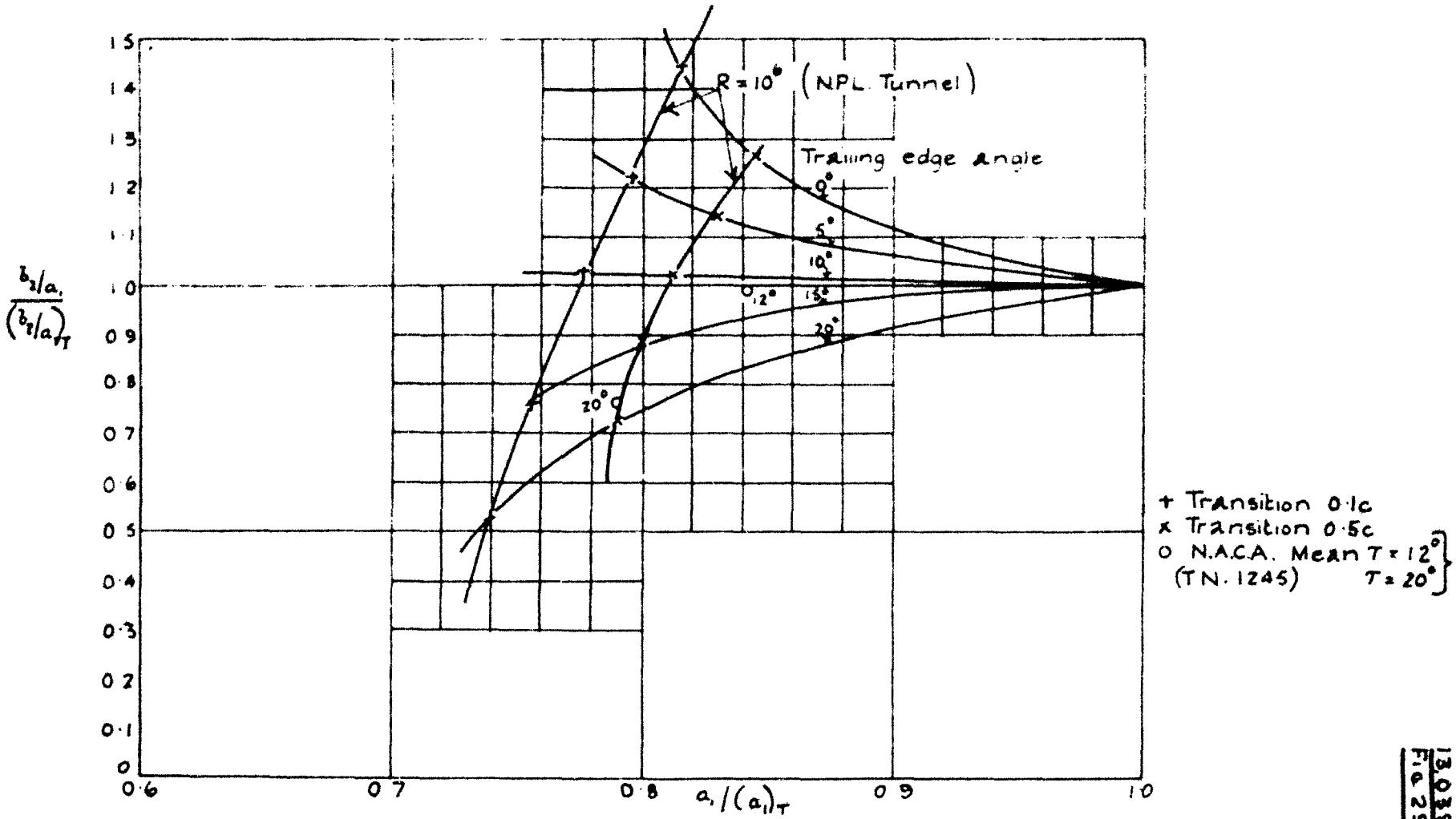

Two dimensional flap hinge - moments. E = 0·4 Chart for b_2/a_1.

13.036
Fig. 29.

FIG 30

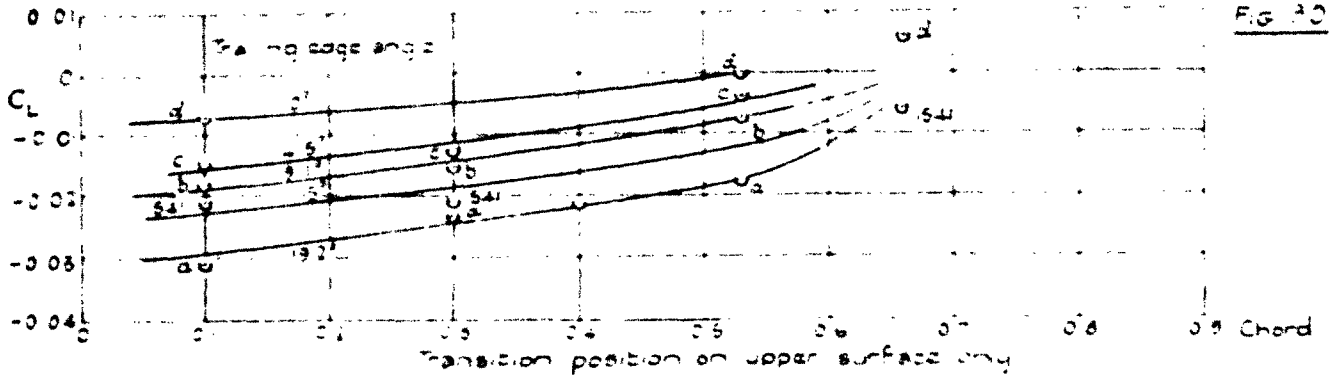

Change of lift with transition movement on one surface only $\alpha = 0°$

FIG 31

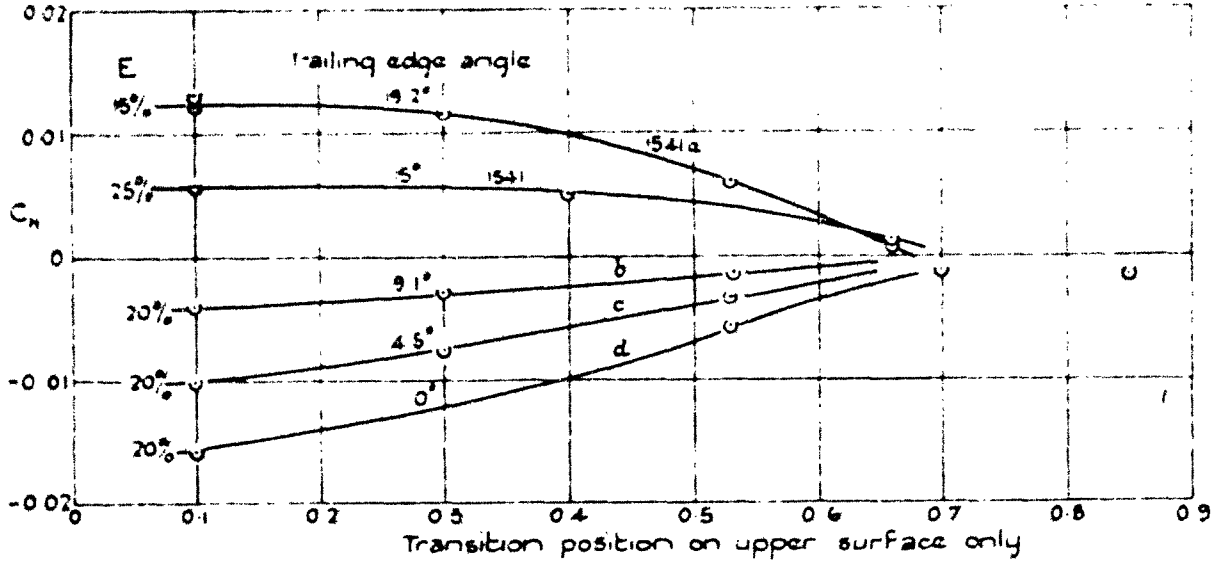

Hinge moment variation with transition movement on one surface only $\alpha = 0°$

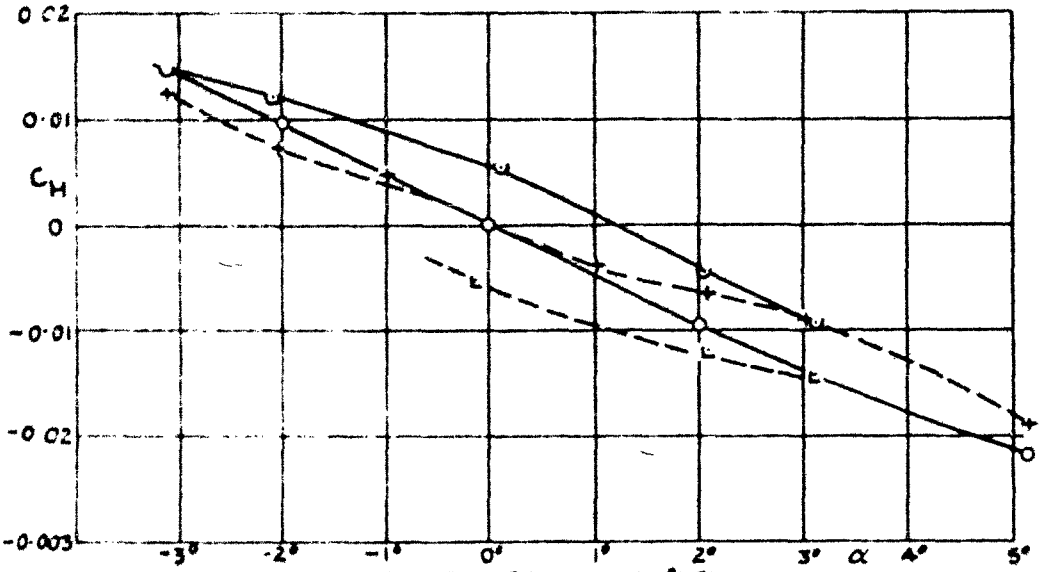

Aerofoil 1541 with 25% Flap.

o No wires
+ Wires at 0·1c on both surfaces
u Wire at 0·1c on upper surface only
L Wire at 0·1c on lower surface only

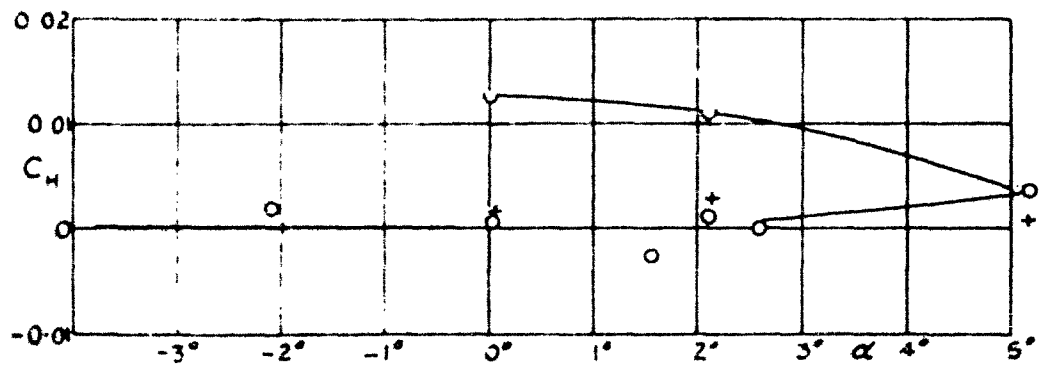

Aerofoil 1541a with 15% flap.

Hinge moments variation with incidence

R.M.

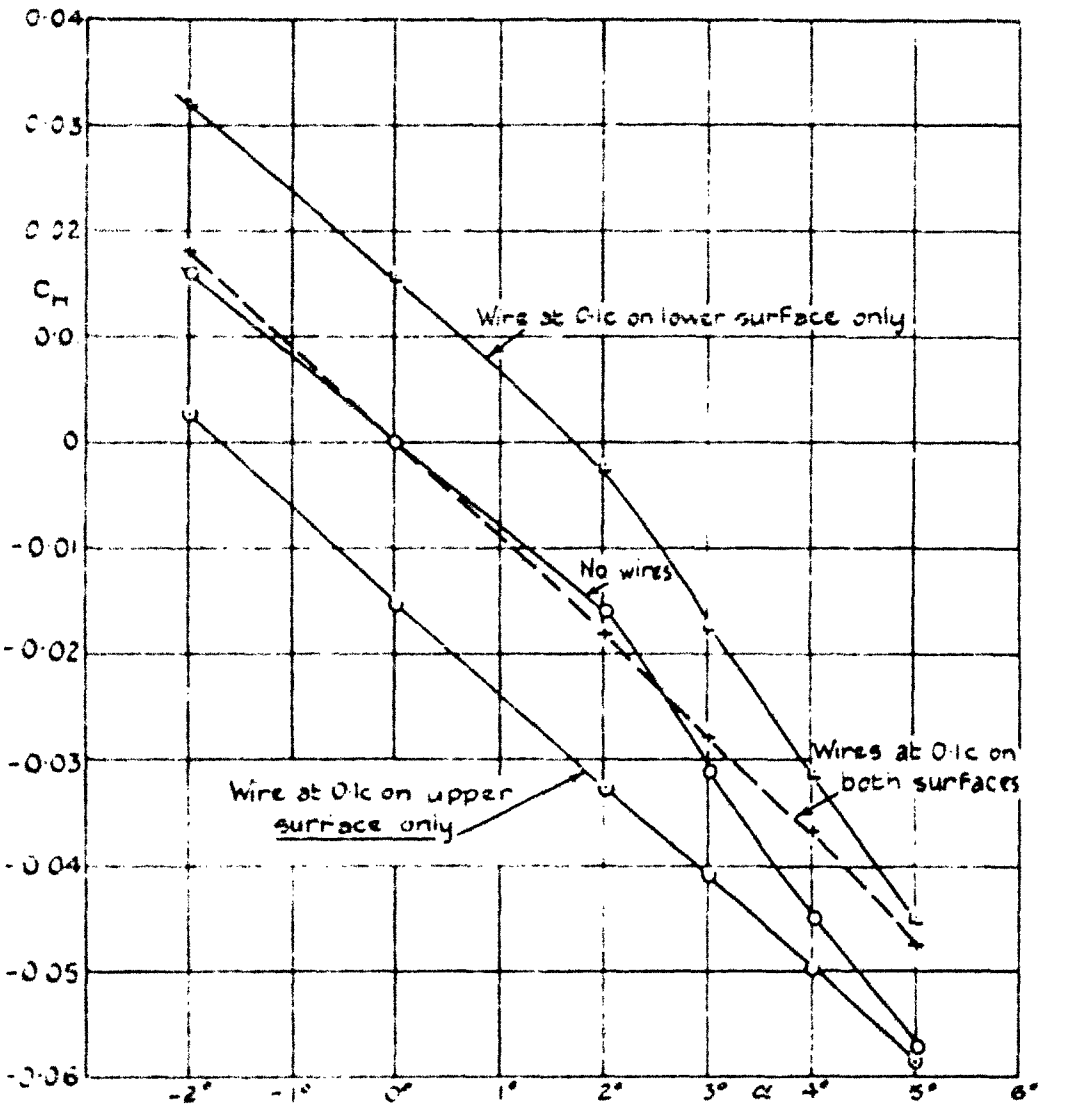

Aerofoil 1541 d with 20% flap Hinge moment variation with incidence.

PM.

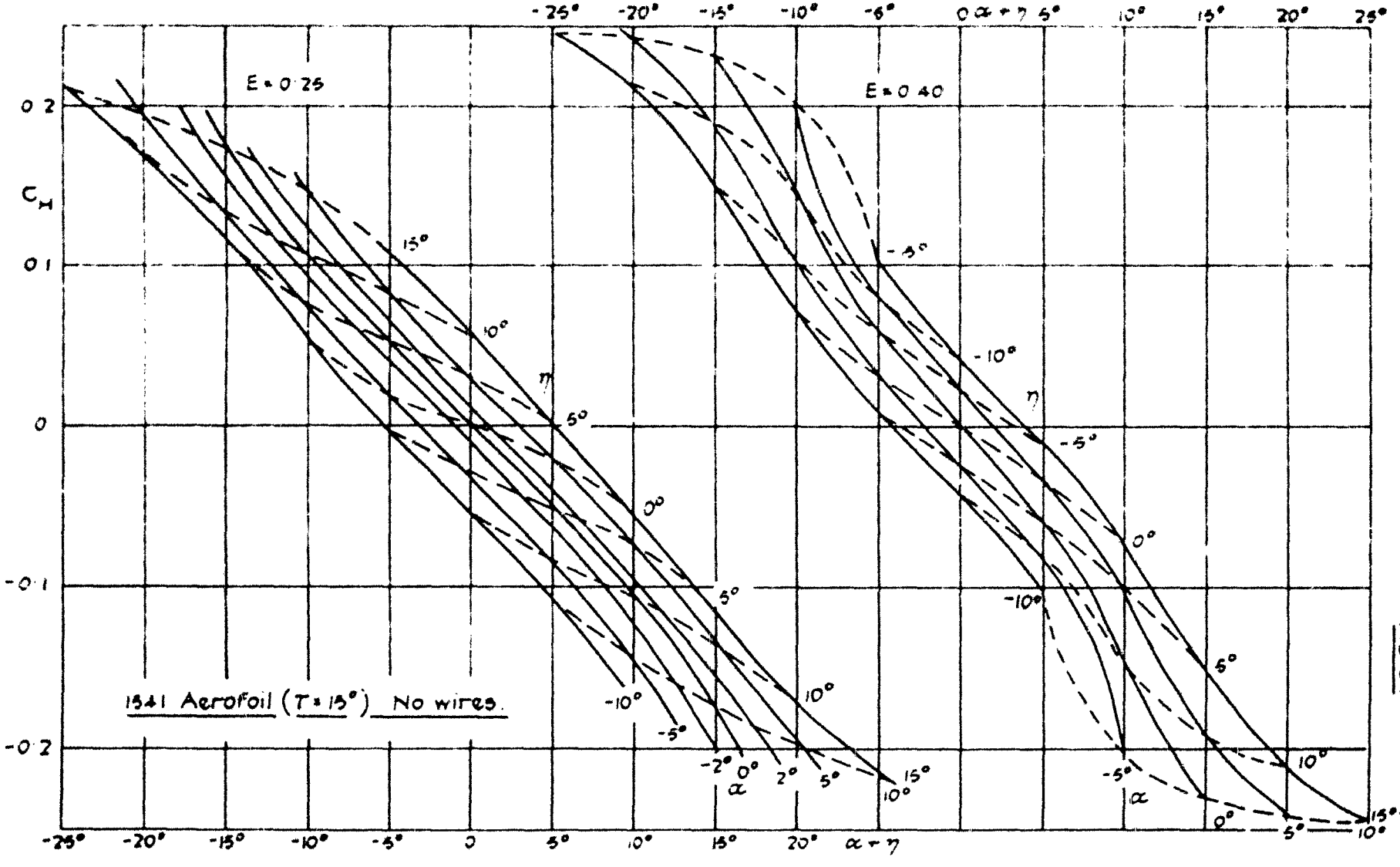
E = 0·25
E = 0·40
C_H
0·2
0·1
0
-0·1
-0·2
-25° -20° -15° -10° -5° 0 5° 10° 15° 20° α + η
15°
10°
5°
0°
-5°
-10°
η
α
-2°
2°
1541 Aerofoil (T = 15°) No wires.

13,059
FIG 34

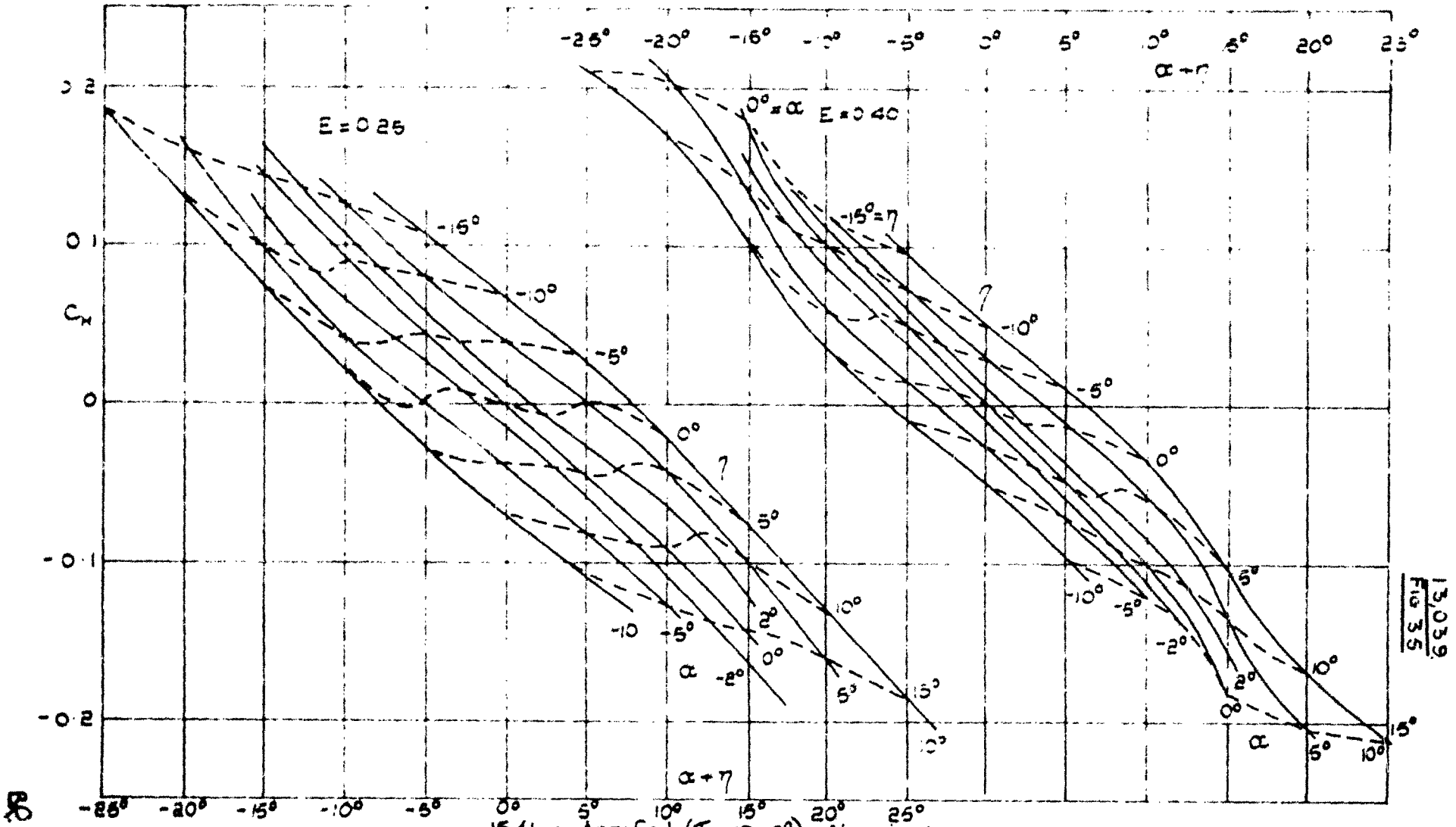

1541 α Aerofoil ($T = 19 \cdot 2°$). No wires.

13,039
FIG 36

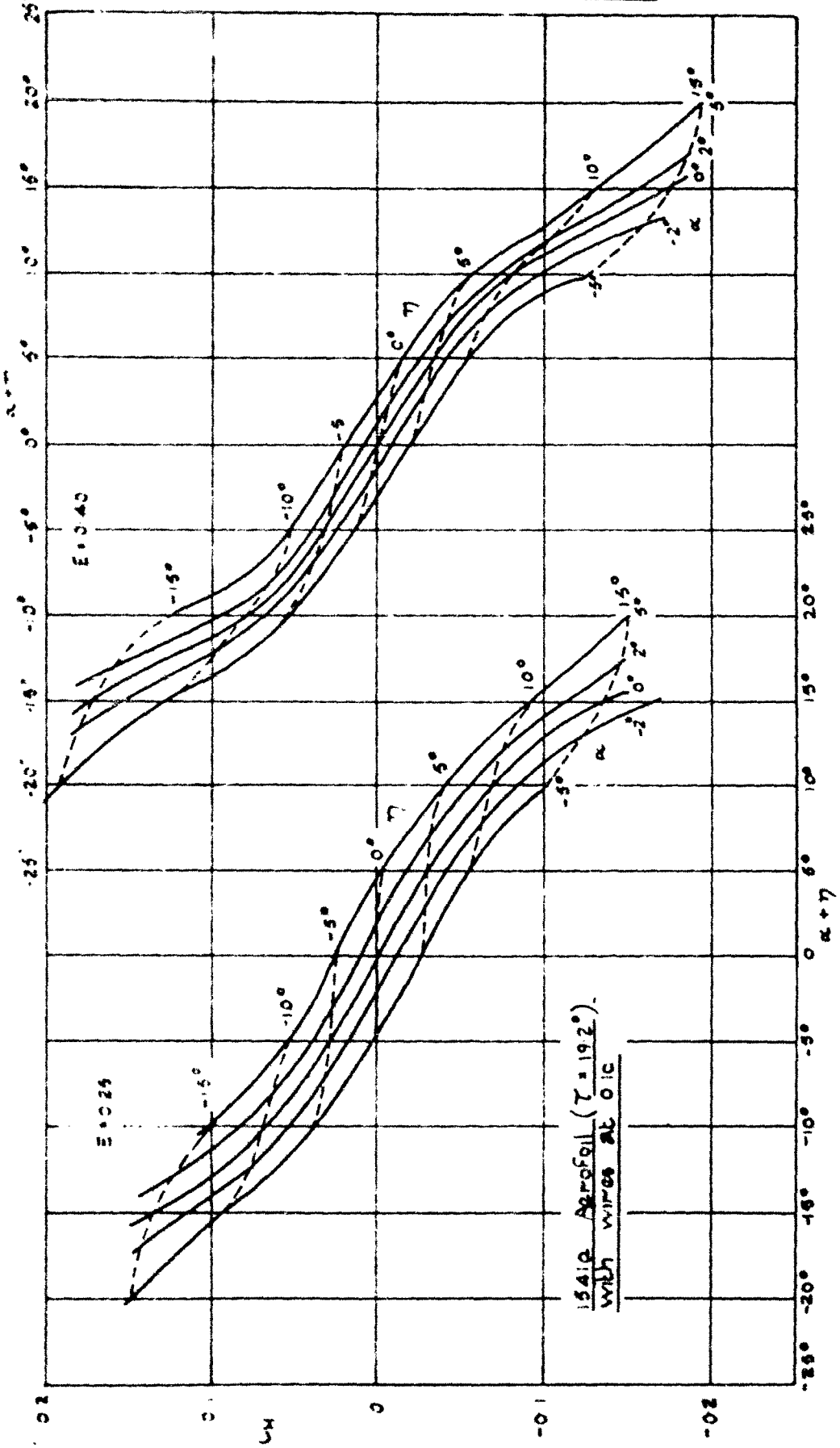
1541a Aerofoil (τ = 19.2°).
With wires at 0·1c
E = 0·40
E = 0·25
α + η
α
η
-15°
-10°
-5°
0°
5°
10°
15°
-2°
2°
-25°
-20°
-15°
-10°
-5°
0°
5°
10°
15°
20°
25°
-0·2
-0·1
0
0·1
0·2
M

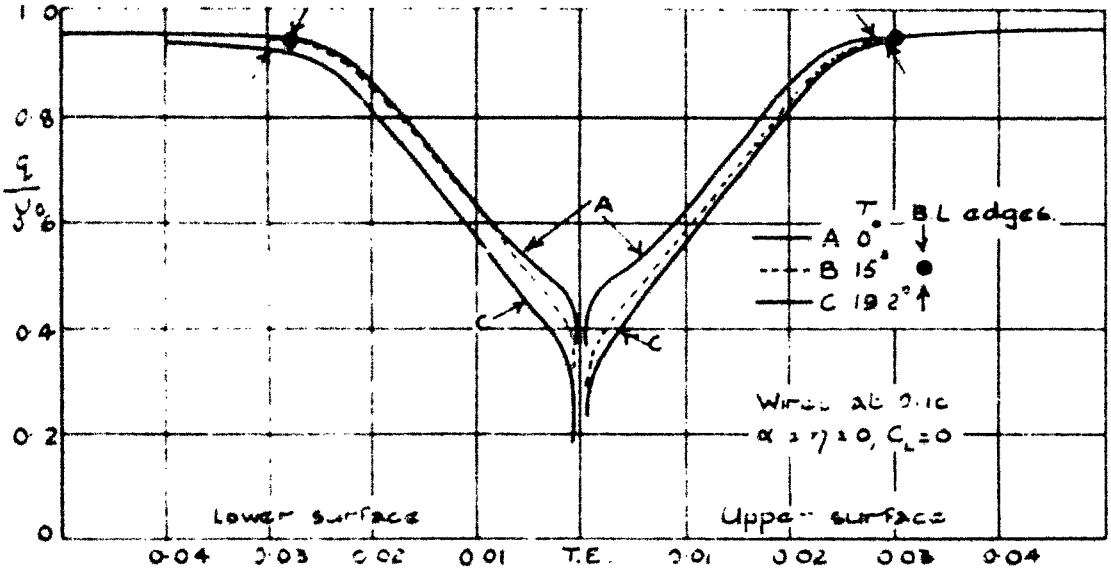

Distance along normal at the trailing edge in terms of the aerofoil chord

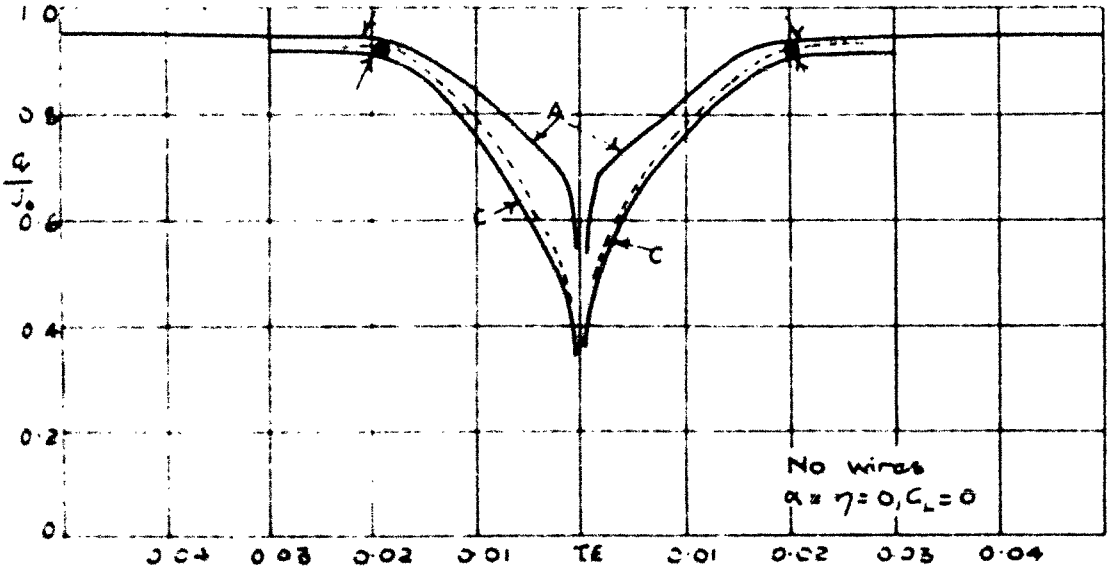

Distance along normal at the trailing edge in terms of the aerofoil chord

Velocities at the traling edge.

MC

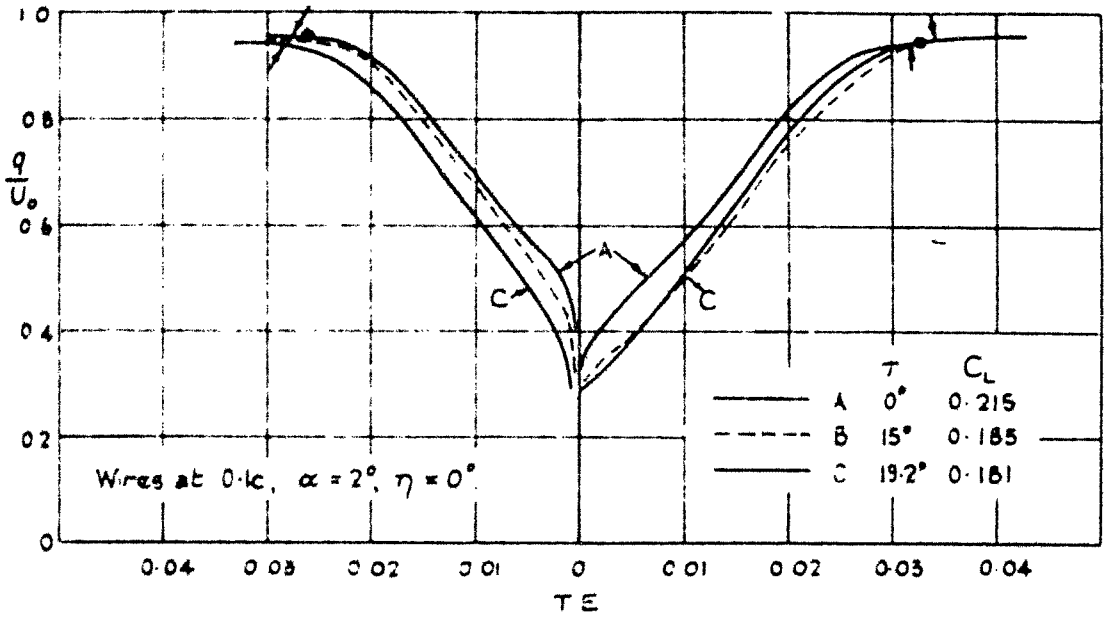

Distance along the normal at the trailing edge in terms of the aerofoil chord.

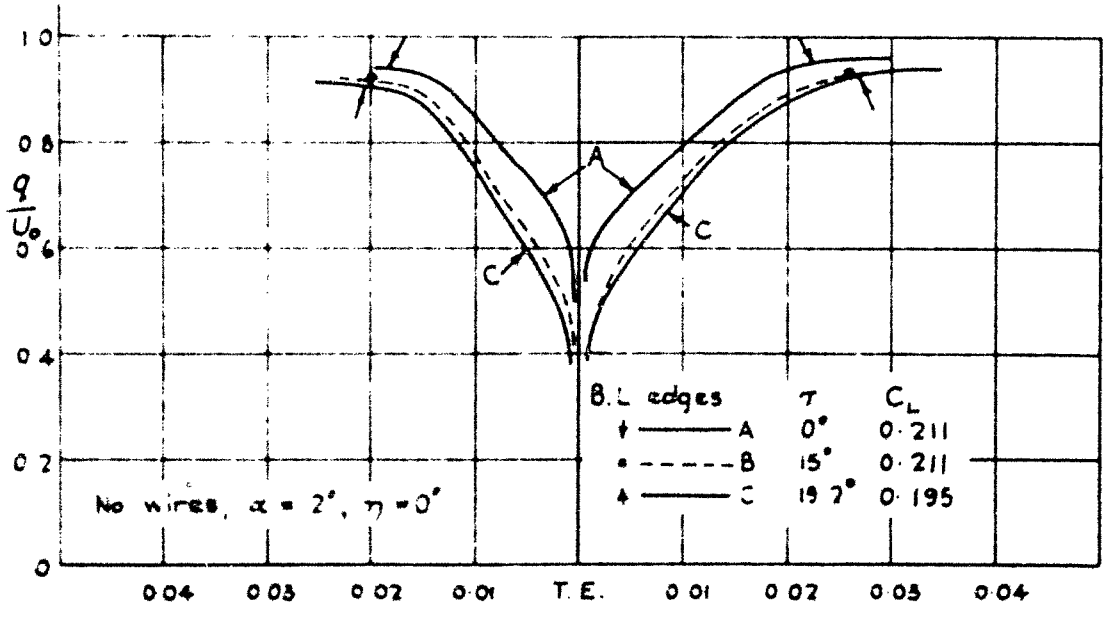

Distance along the normal at the trailing edge in terms of the aerofoil chord

Velocities with trailing edge.

EEM

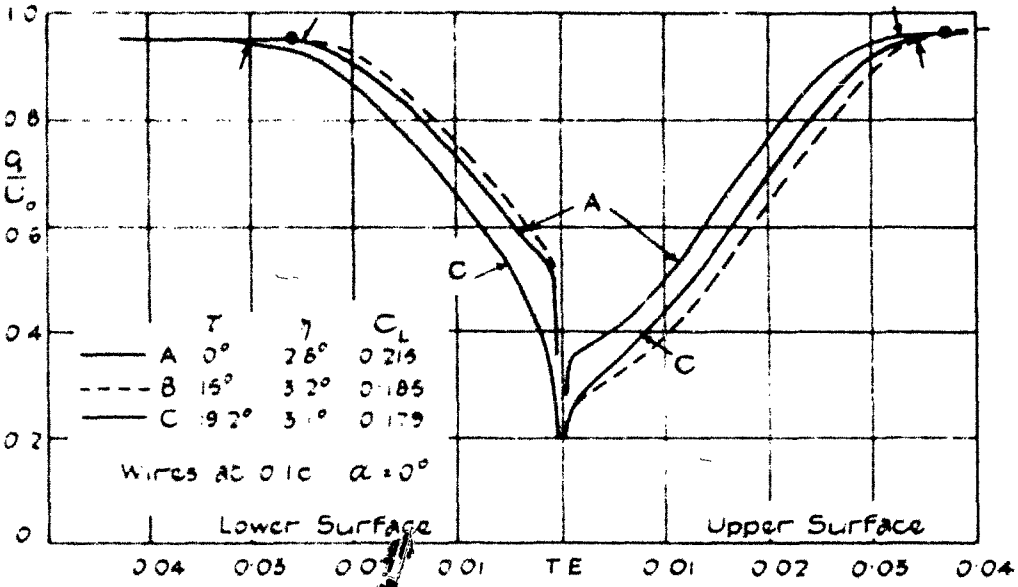

Distance along the normal at the trailing edge in terms of the aerofoil chord

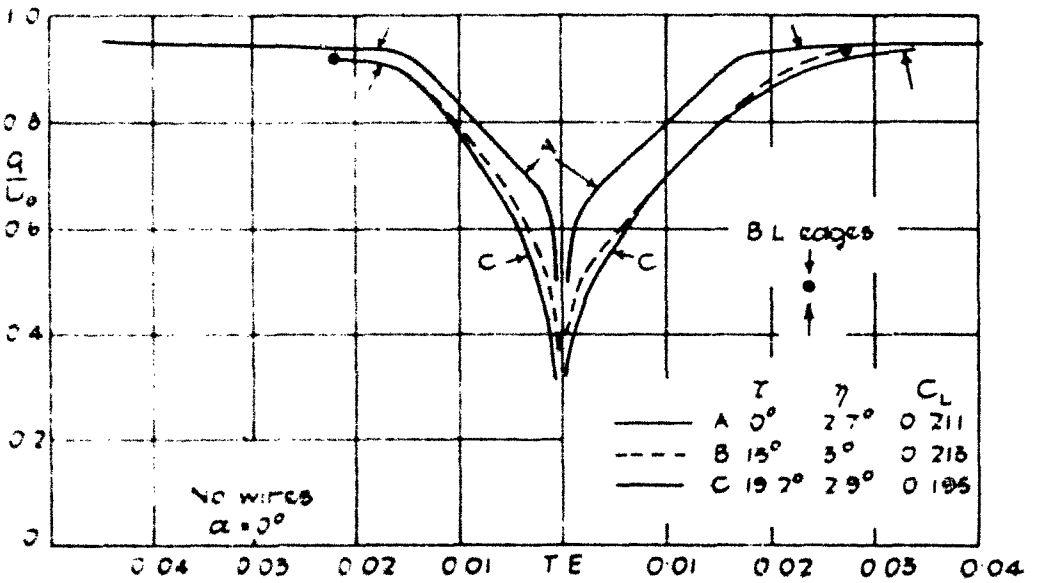

Distance along the normal at the trailing edge in terms of the aerofoil chord

Velocities at the Trailing Edge (40% Flaps).

O.T.

FIG.40

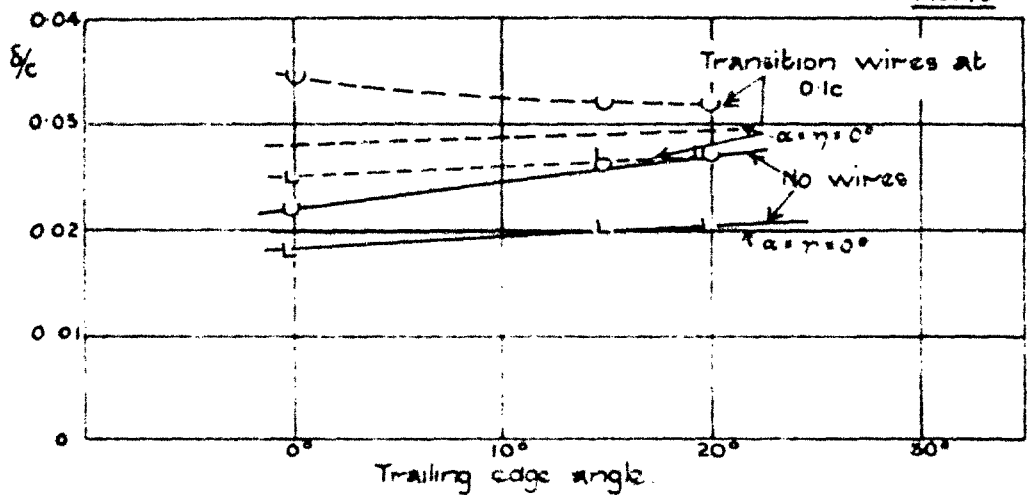

$C_L = 0.19$ $\alpha = 2°$, $\eta = 0°$

U Upper surface
L Lower surface.

FIG.41.

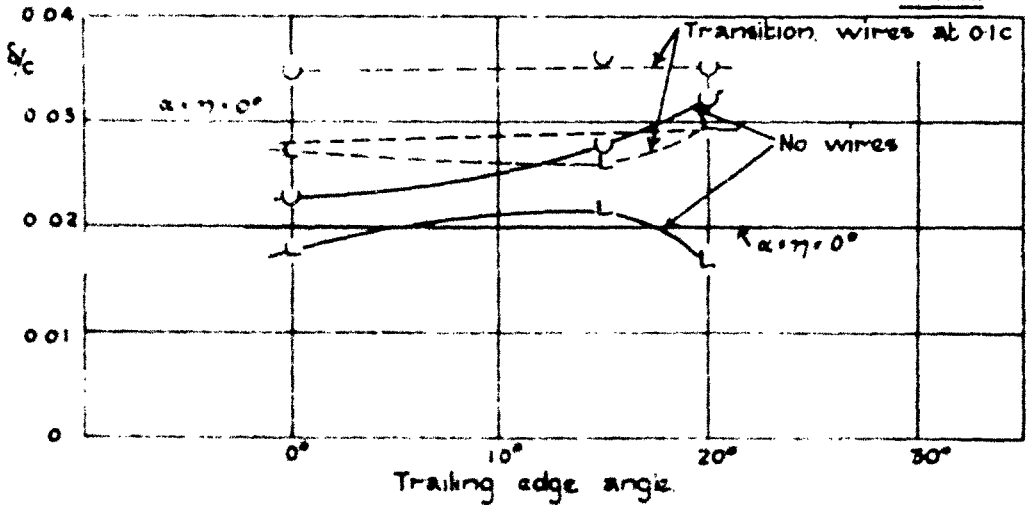

$C_L = 0.19$ $\alpha = 0°$, $\eta = 3.2°$

Boundary layer thickness at the trailing edge.

EPS

Information Centre
Knowledge Services
[dstl] Porton Down
Salisbury
Wilts
SP4 0JQ
22060-6218
Tel: 01980-613753
Fax 01980-613970

Defense Technical Information Center (DTIC)
8725 John J. Kingman Road, Suit 0944
Fort Belvoir, VA 22060-6218
U.S.A.

AD#: AD 011680

Date of Search: 18 November 2008

Record Summary: DSIR 23/18876
Title: Two-dimensional control characteristics: Pt 3
Availability Open Document, Open Description, Normal Closure before FOI Act: 30 years
Former reference (Department) ARC 13039
Held by The National Archives, Kew

This document is now available at the National Archives, Kew, Surrey, United Kingdom.

DTIC has checked the National Archives Catalogue website (http://www.nationalarchives.gov.uk) and found the document is available and releasable to the public.

Access to UK public records is governed by statute, namely the Public Records Act, 1958, and the Public Records Act, 1967.
The document has been released under the 30 year rule.
(The vast majority of records selected for permanent preservation are made available to the public when they are 30 years old. This is commonly referred to as the 30 year rule and was established by the Public Records Act of 1967).

This document may be treated as UNLIMITED.